ABSTRACT

A STUDY OF THE PRODUCTION AND DECAY OF
RESONANT STATES IN PERIPHERAL HIGH ENERGY COLLISIONS

By

Glenn T. Williamson

The current theoretical situation in phenomenological analysis of high energy scattering is reviewed. Various attempts are made to improve upon several models. In particular, the effect of form factors and Regge treatment of propagators on Born amplitudes is examined. Higher order exchange contributions are considered as possible solutions to the problem of energy dependence of higher spin exchange amplitudes. It is found that a combination of the absorptive peripheral model and the Regge pole model is the most successful approach, in that energy dependence difficulties are eliminated as is the need for conspiring trajectories.

A STUDY OF THE PRODUCTION AND DECAY OF RESONANT STATES IN PERIPHERAL HIGH ENERGY COLLISIONS

By

Glenn T. Williamson

A THESIS

Submitted to

Michigan State University

in partial fulfillment of the requirements

for the degree of

DOCTOR OF PHILOSOPHY

Department of Physics and Astronomy

1969

ACKNOWLEDGEMENTS

I wish to thank Professor Hugh McManus for his guidance assistance and support throughout my graduate studies.

I wish to thank Professor Walter Benenson for his critical reading of the manuscript.

My thanks are due to Mrs. Julie Perkins for her assistance in the typing and preparation of this thesis.

TABLE OF CONTENTS

TABLE OF CONTENTS (continued)

LIST OF TABLES

LIST OF FIGURES

LIST OF FIGURES (continued)

LIST OF FIGURES (continued)

LIST OF FIGURES (continued)

INTRODUCTION

In a large class of inelastic elementary particle reactions the experimental data reveal the following prominent general features:

1. One can usually group the final particles into two quasi-states, the center-of-mass of each one nearly maintaining the direction of one of the incident particles, $\frac{d\sigma}{d\Omega_{CM}}$ is strongly peaked either in the forward or backward direction or both.

The reaction ab→1+2+3+...appears as if there were only two particles in the final state. Examples of such reactions are

$$\pi p \to \pi\pi N$$
$$\to \pi\pi\pi N$$
$$KN \to K\pi N$$
$$\to K\pi\pi N$$

We refer to these "particles" as c and d and consider quasi two-body interactions ab→cd in which c or d may be multiparticle states. They are, in fact, the decay products of resonant states and are no different from the resonances themselves kinematically.

The higher the incident particle energy and the simpler the composition of c and d, the more evident the forward or backward peaking becomes.

2. In almost every case, at certain energies the final states do not appear to be directly produced. The reactions proceed via the production of strongly interacting (and very short lived) resonant states which undergo strong decay into the final state. For example

$$\pi N \to \rho N \to \pi\pi N$$

$$KN \to K^*N^* \to K\pi\pi N$$

3. The total cross-section $\sigma_{tot}(s\to\infty)$ behaves like s^{-n} for small positive n. While the density of experimental data available over a wide range of reactions and energies is light, it is possible to note a rapid decrease (in most cases) in the total resonance production cross-section with energy. As we shall see later it is this fact that proves to be the most difficult to handle theoretically.

These are peripheral collisions, and for lack of a better definition we shall call theoretical models for these processes peripheral models. The idea is that a and b do not collide head on; they undergo a glancing collision in which the two particles barely touch each other. We do not expect the trajectories of either of the final particles to deviate from the directions of the incident particles.

One expects these peripheral processes to be dominated by long range forces. Because of the energies involved the treatment must be relativistic and there is no reason to suppose that we can ignore the intrinsic spin of the particles. From the point of view of field

theory these reactions proceed via the exchange of the virtual quanta that will induce the longest range force, the quanta of lightest mass. The problem has been reduced to consideration of a sum of one particle exchange graphs as indicated in Figure 1.

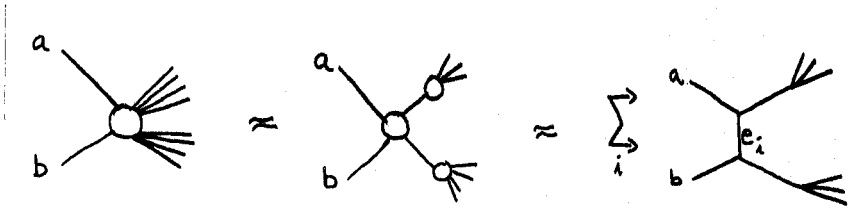

Figure 1. The reaction ab→n particles in the region where the final state is dominated by production of two resonances is approximated by a sum over all allowed one-particle exchanges.

In its simplest form, this "Born Term Model" leads to a matrix element of the form

$$\langle cd|B|ab\rangle = B_{aec}(t,m_c)\frac{p}{t-m_e^2}B_{bed}(t,m_d)$$

for the production of the intermediate resonant states where $t=-(b-d)^2$ is the invariant 4-momentum transfer, $p/(t-m_e^2)$ is the propagator of the exchanged particle and $B_{\ell en}(t,M_n)$ is the vertex function. At $t=M_e^2$, $B_{\ell en}(M_e^2, M_n^2)$ is the matrix element for the physical process $\ell+e\to n$. If one regards n as a particle, B is equal to the (ℓen)-coupling constant multiplied by a known kinematical factor.

These vertex functions are obtained in the usual way from interaction Lagrangians or by writing down the most general function consistent with Lorentz invariance and then using hermiticity, CPT and other strong interaction invariances to limit the form further.

Since small physical values of t correspond to small center-of-mass scattering angles it is clear that if the vertex functions are not pathological in their behavior this Born approximation ought to be a good start to explaining peripheral collisions. And because of the "factored" structure of $\langle cd|B|ab\rangle$ we have a basic test of the model: $\frac{d\sigma}{d\Omega}$ should be independent of the angle between the planes defined by ac and bd.

The Exchanged Particle

Consider any specific reaction and the usual invariance principles determine which exchanges are allowed.

Example: $KN \rightarrow KN^*$

1. Conservation of baryon number tells us that e cannot be a baryon.

2. None of K,N,N* are eigenstates of the G-parity operator so we obtain no specific information from G-parity conservation: G_e is arbitrary.

3. Since strangeness is conserved at both vertices the exchanged particle must not be strange: $S_e=0$.

4. Isotopic spin conservation at the NeN* vertex requires $1/2+I=3/2$, which gives $I_e=1,2$. Consistency with the KeK vertex requires that the exchanged quanta be a member of an I-spin triplet: $I_e=1$.

5. Consider angular momentum and parity conservation at the KeK vertex in the outgoing K-meson rest frame. The K has $J^P=0^-$ so the addition theorem requires $0^-+\ell(-)^{\ell}+J^P_e=0^-$. This reduces immediately to $\ell(-)^{\ell+1}+J^P_e=0^-$. Clearly we must have $\ell=J_e$ and $p_e=(-)^{\ell}=(-)^{Je}$ which means that $J^P_e=0^+$ or $1^-,2^+,\ldots$ Examination of the NeN* vertex provides no information which further restricts J^P_e.

In summary, for KN→KN* the exchanged quanta must be a non-strange member of an isospin triplet of mesons with $J^P=J(-)^J$. We choose from among the known low lying meson states and conclude that ρ exchange is likely to dominate.

One proceeds in just this way, applying the conservation laws at each vertex in turn for each reaction to be considered. This procedure rarely limits the exchanged quanta to a single state.

Decay of the Resonant State

Recall that particles c, d or both in the reaction ab→cd are in most cases pseudo-particles, resonant interactions of several elementary particles. So far we have discussed in general terms the amplitude $\langle cd|M|ab\rangle$ for the production of the resonant state, particle d. (For the moment c will be just another elementary particle, eg. πN→πN*). We will consider decay into two particles: d→fg.

If we had particle d, with spin s_d at rest in the laboratory, its decay would be governed solely by the transition matrix for the process d→fg:

$$\left(\frac{d\sigma}{d\Omega}\right)_{decay} \sim \Sigma_{fgd} |\langle fg|M|d\rangle|^2.$$

Given an ensemble of states d at rest with spin polulation λ_d we have no reason to expect that the populations of each projection state are different. It is clear that this is not the case in our situation. We do not start with particle d; we actually observe the process ab→cfg which proceeds via the intermediate state d: ab→cd→cfg. In contrast to the above, we do not expect the resonance d to be produced with an isotropic spin distribution. It must be assumed that the production matrix elements are spin dependent until we know otherwise. One can still obtain the decay angular distribution from the formula given above, but the initial state for the decay matrix element must be weighted by the probability for production of the spin state

$$\langle fgc|M|ab\rangle = \Sigma_{spin} \langle fg|M_{decay}|d\rangle\langle cd|M_{prod.}|ab\rangle$$

and therefore

$$\left(\frac{d\sigma}{d\Omega}\right)_{d\to fg} \sim \Sigma \langle fg|M_d|d\rangle^* \langle fg|M_d|d'\rangle \Sigma_{cab} \langle cd|M_p|ab\rangle^* \langle cd'|M_p|ab\rangle$$

Considering only the angular part H of the decay matrix element and normalizing, we arrive at a formula for the expected angular distribution of the decay products f, g of the resonance d produced in ab→cd. For convenience everything is done in the d rest frame.

$$W(\alpha,\beta) = N \Sigma H(fgd)^* H(fgd') \rho_{dd'}$$

$$\text{where } \rho_{dd'} = N_2 \Sigma \langle cd|M_\rho|ab\rangle^* \langle cd'|M_\rho|ab\rangle$$

$$T_r \rho = 1 \text{ determines } N_2$$

Various symmetries can be used to obtain relations among the production density matrix elements $\rho_{mm'}$. To find these it is necessary to examine $W(\alpha,\beta)$ in more detail.

Coordinate system

Since it is convenient to do calculations in the center-of-mass frame, we start there. In all of our calculations we have defined the production plane to be the XZ plane with the momentum vectors aligned as shown in Figure 2.

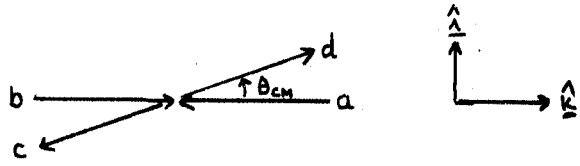

Figure 2. The two-body scattering ab→cd in the center-of-mass and the orientation of the x and z axes.

Because it is easiest to look at the decay of d from its rest system, we perform a Lorentz transformation into this system as indicated in Figure 3.

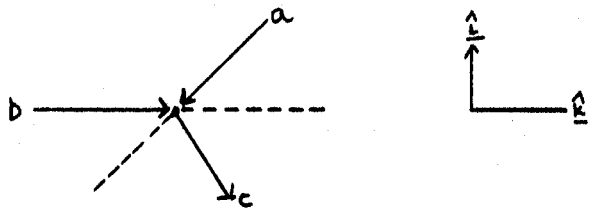

Figure 3. The two body scattering ab→cd in the rest frame of particle d.

The $\underline{j}$ direction, the normal to the production plane, is defined by $\underline{j} = \frac{\underline{a}\times\underline{c}}{|\underline{a}\times\underline{c}|}$.

The decay angular distribution

Now add the decay products f and g to the diagram, and delete a and c to get them out of the way as indicated in Figure 4.

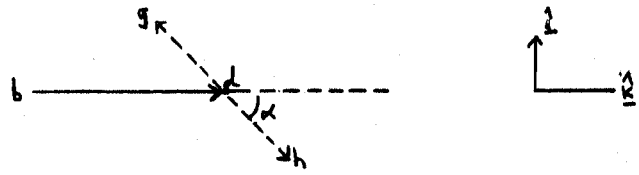

Figure 4. The decay products g and h of the resonance d in its rest frame.

Two angles are needed to locate the decay products. Momentum conservation requires f and g to move in opposite directions. We use a polar angle α, which measures deviation of the line of motion from the $\underline{k}$ direction, and an azimuthal angle β measuring deviation from the production plane. These definitions correspond to the usual defining angles for the spherical harmonics $Y_{\ell m}(\alpha,\beta)$. As long as we choose the $\underline{k}$ axis to be the spin quantization axis for the resonant state d of spin j_d, the angular part of the decay matrix element will be $|\ell m\rangle$ coupled to j_f+j_g to form j_d.

An Example:

This is a $1^- \to 0^- + 0^-$ transition. In the ρ rest frame the intrinsic spin of the ρ meson becomes the relative orbital angular momentum of the two pions. The angular part of the decay matrix element is proportional to $Y_{\ell m}(\alpha,\beta)$. We write

$$W(\alpha,\beta) \sim \Sigma_{mm'} Y_{1m}(\alpha,\beta) Y^*_{1m'}(\alpha,\beta) \rho_{mm'}$$

where we normalize $\int d\Omega_{\alpha\rho} W(\alpha,\beta) = 1$.

Symmetries of $\rho_{mm'}$

It is useful to take advantage of available symmetries to simplify the density matrix as much as possible. We require that ρ be hermitian, $\rho^+ = \rho$. Application of parity conservation to $ab \to cd$ leads to additional relations among the production amplitudes. Substitution of these relations into the formula for ρ immediately shows that

$$\rho_{mm'} = (-)^{m-m'} \rho_{-m-m'}$$

These two relations plus the trace condition enable us to write

$$\rho^{J=1}_{mm'} = \begin{bmatrix} 1/2(1-\rho_{00}) & \rho_{10} & \rho_{1,-1} \\ \rho^*_{10} & \rho_{00} & -\rho^*_{10} \\ \rho_{1,-1} & -\rho_{10} & 1/2(1-\rho_{00}) \end{bmatrix}$$

Using this matrix we obtain an expression for $W^{\rho\to 2\pi}(\alpha,\beta)$:

$$W^{i\ 0+0}_{(\alpha,\beta)}=\frac{3}{4\pi}[3/2(1-\rho_{00})+1/2(3\rho_{00}-1)\cos^2\alpha-\rho_{1,-1}\sin^2\alpha\cos 2\beta - \sqrt{2}R_e\rho_{10}\sin 2\alpha\cos\beta]$$

One also obtains an expression for the polarization of particle d by using $P=Tr\rho J_d$. P_x and P_z are found to vanish, so the polarization vector of d is perpendicular to the production plane.

The decay of a spin j_d into spins j_f and j_g can be analyzed in a similar way but it is necessary to use the angular momentum addition theorem to write the proper angular functions. Once one has an expression for W in terms of density matrix elements, he again examines the effect of invariances at the vertices on the density matrix elements to obtain model dependent predictions for the angular distributions, assuming a j^p_e for the exchanged quantum. To show the method and complete the ρ-production example, we look at the $\rho\to\pi\pi$ decay.

Assume the dominant contribution to $\pi N\to\rho N$ is the pion exchange force and ask what this means for the decay distribution of the produced mesons. Consider the vertex in the ρ-meson rest frame.

A unit of orbital angular momentum is picked up in ρ-formation as intrisic spin and j_z for the 2π system is zero. Note that parity is conserved. Conservation of J_z implies $J_z=0$ and the $j_z=1$ spin projections of the ρ are not produced at all. The only non-vanishing density matrix

element is ρ_{00} which, because of the normalization condition, must be unity. Substitution into $W(\alpha,\beta)$ gives

$$W(\alpha,\beta) = 3/4\pi\cos^2\alpha \qquad W(\alpha) = \int d\beta W(\alpha,\beta) = 3/2\ \cos^2\alpha$$

$$W(\beta) = 1/2\pi$$

We look for this behavior in the experimental data as evidence for π-exchange. This result is quite general; any reaction of the form PB→VB proceeding via pseudoscalar exchange will lead to the above angular distributions for the decay of the produced V-meson.

Similar analyses may be performed for the other allowed spin-parity assignments of the exchanged quanta and for arbitrary spin of the produced resonance. Table A summarizes the results of analyses for other relevant cases.

When doing calculations helicity eigenstates are used rather than spinors quantized relative to the z-axis.[1] These are states in which each spin is quantized relative to its own direction of motion. Such states have very simple Lorentz transformation properties making them very easy to use. We calculate amplitudes and cross-sections in the production center-of-mass system and decay angular distributions in the decay center-of-mass system. Before we can use the density matrix it is necessary to perform a rotation so that spin quantization is relative to the z-axis, a more transparent situation for comparison with experiment.

In the production CM, the angle of rotation for c,d is clearly θ_{cm}. In the c(d) rest system we have

$$\sin\psi_c = \frac{q}{a_c}\sin\theta_{cm} \qquad (\sin\psi_d = \frac{q}{b_d}\sin\theta_{cm})$$

where, with $\lambda(x,y,z) = x^2+y^2+z^2-2xy-2xz-2yz$

$q = \frac{1}{2\sqrt{s}}\lambda^{1/2}(s,m_a^2,m_b^2)$ = incident channel CM momentum production process

$a_c = \frac{1}{2m_c}\lambda^{1/2}(t,m_a^2,m_c^2)$ = momentum of a in c rest system

$b_d = \frac{1}{2m_d}\lambda^{1/2}(t,m_b^2,m_d^2)$ = momentum of b in d rest system

This transformation formula for the angle is very easy to derive. The component of a 4-vector perpendicular to the direction of a Lorentz transformation is unaffected by that transformation.

Let $\hat{\rho}^{(J_c)}_{\lambda_c\lambda'_c}$ be the helicity state density matrix for production of the resonant state c of spin j_c. The density matrix for quantization along the Z-axis in the c rest system is then given by

$$\rho^{(J_c)}_{\lambda_c\lambda'_c} = d^{J_c}_{\lambda_c\lambda_1}(\psi_c)\ \hat{\rho}^{(J_c)}_{\lambda_1\lambda'_1}\ d^{J_c}_{\lambda'_1\lambda_1}(-\psi_c)$$

which is a function of s and t for the production process. It is this $\rho_{mm'}$ that goes into the angular distribution formulas.

A look at the experimental data provides clues to the production mechanism. We invent a model, calculate production angular distributions, total cross-sections, production density matrix elements, and compare with the experimental data. Proceeding in this manner, it has been possible to explain a large number of high energy reactions, though in most cases not without modifications, to the basic Born Terms.

TABLE I

Predictions of the BTM for Density Matrix Elements

1. Vector Meson Production ($J^P=1^-$) [decay: $1^-\to 0^-+0^-$]
   significant density matrix elements: $\rho_{00}, \rho_{1,-1}, \rho_{10}$
   (ρ_{10} is complex).
   a) Pseudoscalar exchange ($J^P=0^-$)
      prediction: $\rho_{00}=1$, others zero.
   b) Natrual parity exchange ($J^P=J^{(-)^J}$)
      prediction: $\rho_{1,-1}$ arbitrary, others zero.
   c) Unnatural parity exchange ($J^P=J^{(-)^{J+1}}$)
      no prediction.

2. N^*_3 production ($J^P=3/2+$) [decay: $3/2^+\to 1/2^++0^-$]
   significant density matrix elements: $\rho_{33}, \rho_{3-1}, \rho_{31}$
   ($\rho_{3,-1}, \rho_{31}$ complex)
   a) Pseudoscalar exchange ($J^P=0^-$)
      Prediction: all above elements are zero.
   b) Vector meson exchange ($J^P=1^-$)
      prediction: $\mathrm{Re}\rho_{31}=0$, $\rho_{33}=3/8$, $\mathrm{Re}\rho_{3,-1}=3/8$.

THE GLAUBER FORMALISM FOR HIGH ENERGY SCATTERING AND THE BORN APPROXIMATION

We start with a potential $V(\underline{r})$ of finite range and use the Schroedinger equation to solve for the wave function, assuming high energy for the incident particle. By high energy we mean the incident particle energy ε is much greater than the absolute magnitude of the potential V_0, and that the wave length is much shorter than the range r_0 of the potential:

$$V_0 << \varepsilon \quad kr_0 << 1.$$

Since, relative to ε the potential is weak, we do not expect the wave function to deviate significantly from a plane wave. We write

$$\chi(\underline{r}) = e^{i\underline{k}\cdot\underline{r}} M(\underline{r}).$$

M is assumed to vary slowly with $\underline{r}$.

Substituting in the integral form of the Schroedinger equation

$$\psi(\underline{r}) = e^{i\underline{k}\cdot\underline{r}} - \lambda \int \frac{e^{ik|\underline{r}-\underline{r}'|}}{|\underline{r}-\underline{r}'|} V(\underline{r}')\psi(\underline{r}')d\underline{r}',$$

we easily obtain

$$M(\underline{r}) = 1 - \lambda \frac{e^{ik|\underline{r}-\underline{r}'| - i\underline{k}\cdot(\underline{r}-\underline{r}')}}{|\underline{r}-\underline{r}'|} V(\underline{r}')M(\underline{r}')d\underline{r}'$$

$$= 1 - \lambda \int \frac{e^{i(kr_1 - \underline{k}\cdot\underline{r}_1)}}{r_1} V(\underline{r}-\underline{r}_1)M(\underline{r}-\underline{r}'_1)d\underline{r}_1$$

where $d\underline{r}_1 = r_1^2 dr_1 d(\cos\theta) d\rho$.

Assuming $V_0 M$ changes appreciably over distance d but varies slowly over a wave length, we obtain by partial integration

$$M(\underline{r}) = 1 + \lambda \int dr_1 r_1^2 d\theta \left[\frac{e^{ikr_1(1-\cos\theta)}}{ikr_1} V(\underline{r}-\underline{r}_1) M(\underline{r}-\underline{r}_1) \right]_{\cos\theta=-1}^{\cos\theta=1} + \theta\left(\frac{1}{kd}\right)$$

At $\mu = -1$ (r_1 antiparellel to k) the exponential oscillates rapidly and this term is also of order 1/kd. The leading contribution is

$$M(\underline{r}) = 1 - i\frac{\lambda}{k} \int dr_1 V(\underline{r}-\underline{r}_1) M(\underline{r}-\underline{r}_2) \Big|_{\underline{r}_2 \wedge \underline{k}}^{\underline{r}_1 || \underline{k}}$$

Choosing $\underline{k}$ to be in z direction we obtain

$$M(\underline{b},z) = 1 - i\lambda/k \int dz' V(\underline{b}+\hat{\underline{k}}z) M(\underline{b}+\hat{\underline{k}}z')$$

$$= \frac{dM}{M} = -\frac{\lambda}{k} V dz' \rightarrow M(\underline{b},z) = e^{-i\lambda/k \int_{-\infty}^{z} dz' V(\underline{b}+\hat{\underline{k}}z')}$$

where we have used as boundary condition $M(\underline{b}, z=-\infty) = 1$, which comes from the requirement that we start with an incident plane wave.

The final form for the wave function is

$$\chi(\underline{b},z) = e^{i\underline{k}\cdot(\underline{b}+\hat{\underline{k}}z) - i\lambda/k \int_{-\infty}^{z} dz' V(\underline{b}+\hat{\underline{k}}z)},$$

which is valid in the region of the potential.

The limits of applicability of this approximation have been given by R. J. Glauber.[2] It is sufficient to know that this formalism will provide a good description of the scattering in the forward and backward cones. We

use the wave function $\chi(\underline{b},z)$ in the formula for the scattering amplitude in place of a plane wave. The idea is that if the potential is well-behaved and the incident energy is high enough, the incident wave will be only slightly distorted in the region of the potential. We have calculated the first order correction to the wave function due to this distortion. This is called the Distorted Wave Born Approximation and was used by J. D. Jackson and collaborators[3,4] as the starting point in developing the absorptive model.

ABSORPTIVE CORRECTIONS

We are studying inelastic processes of the form ab→cd, which we assume to be due to the interaction V in lowest order. Now we allow a and b to interact elastically before they interact via V to produce c and d, which also interact elastically, as shown in Figure 5.

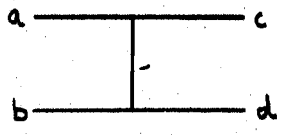

Figure 5. The absorptive model diagram for the scattering ab→cd.

The incident and outgoing channel elastic interactions V_i and V_f are treated exactly. The result is a modification to the Born term for the inelastic process. At the interaction V, a and b are no longer plane waves; they are gradually distorted by the elastic interaction as they approach the inelastic interaction region. We require that V_i and V_f and the incident energy satisfy the restrictions implied in the Glauber wave function. The incident and final wave functions χ_i and χ_f are

$$\chi^*_f(\underline{b},z)=e^{-i\underline{q}'\cdot\underline{r}_e-i\lambda/q\int_z^\infty dz' V_f(\underline{b}+\hat{\underline{k}}z)}$$

$$\chi_i(\underline{b},\underline{z})=e^{i\underline{q}\cdot\underline{r}_e-i\lambda/q\int_{-\infty}^{z} dz' V_i(\underline{b}+\hat{\underline{k}}z')}$$

We use these wave functions to calculate first order contribution to the inelastic scattering:

$$\langle cd|M|ab\rangle \simeq \int d^2b dz e^{i\underline{\delta}\cdot\underline{b}} \langle cd|V|ab\rangle e^{-i\lambda/q\int_{-\infty}^{z} dz' V_i - i\lambda/q'\int_{z}^{\infty} dz' V_f}$$

$$\simeq 2\pi\int_0^\infty b db J_0(\delta b) e^{i/2\chi_i(b)} B(b) e^{i/2\chi_f(b)}$$

where $B(b)=\int_{-\infty}^{\infty} dz V(\underline{b}+\hat{\underline{k}}z)$ and $\underline{\delta}=\underline{q}-\underline{q}'$

The range of V is assumed much smaller than V_i or V_f and the phase shift of wave traveling through V at impact parameter b is given by

$$\chi_n(b) = -\frac{\lambda}{q_n}\int_{-\infty}^{\infty} dz' V(\underline{b}+\hat{\underline{k}}z) \qquad (n=i,f)$$

Compare this expression for the amplitude with the partial wave expansion.

$$\langle|M|\rangle = \sum_{\ell}(\ell+1/2)M_\ell P_\ell(\cos\theta) \simeq \int x dx M(x) J_0(\omega x) \qquad (\omega=2\sin\theta/2)$$

Note that the expansion in impact parameter is approximately equivalent to the partial wave expansion.

To obtain a relativistic version of this formula and include spin, we assume that the partial Born amplitude $\langle\lambda_c\lambda_d|M^j|\lambda_a\lambda_b\rangle$, where λ_i is the helicity of the 1^{th} particle, is replaced by $e^{i/2\chi_I^J} M^j e^{i/2\chi_F^j}$.

We start with the relativistic partial wave expansion

$$\langle\lambda_c\lambda_d|M|\lambda_a\lambda_b\rangle = \sum_j (j+1/2)\langle\lambda_c\lambda_d|M^j|\lambda_a\lambda_b\rangle d^j_{\lambda\mu}(\theta), \quad {}^{\lambda=\lambda_a-\lambda_b}_{\mu=\lambda_c-\lambda_d}$$

invert it to obtain M^j

$$\langle\lambda_c\lambda_d|M^j|\lambda_a\lambda_b\rangle = \int d(\cos\theta)\langle\lambda_c\lambda_d|M|\lambda_a\lambda_b\rangle d^j_{\lambda\mu}(\theta).$$

Including the distorted wave correction DW_j and resumming the series we obtain

$$\langle\lambda_c\lambda_d|M'|\lambda_a\lambda_b\rangle=\sum_j(j+1/2)\{DW_j\int d(\cos\theta)\langle\lambda_c\lambda_d|M|\lambda_a\lambda_b\rangle d^j_{\lambda\mu}(\theta)\}d^j_{\lambda\mu}(\theta').$$

In actual practice this procedure is avoided whenever possible by making use of a few mathematical tricks. For single-quantum exchanges, retaining only the two lowest terms in $n=|\mu-\lambda|$, the amplitudes can be put in the form

$$M^a_n=\theta\ \frac{1}{t-m_e^2}\ (\chi_{an}\omega^n+\bar{\chi}_{an}\omega^{n+2}).$$

It is possible to write

$$\frac{1}{t-m_e^2}=\frac{1}{qq'}\ \frac{1}{\varepsilon^2+\omega^2}$$

where ε^2 is composed of angle independent kinematical quantities. Then using

$$\frac{\omega^n}{\varepsilon^2+\omega^2}=\varepsilon^n\int_0^\infty xdxJ_n(\omega x)k_n(\varepsilon x)$$

we are able to write each amplitude as a partial wave sum and all that need be done is to insert the distorted wave factor DW(X) under the integral.

It should be mentioned that for all of these high energy reactions, large numbers of partial waves contribute. Since we are limited to small θ_{CM} we can make use of the approximation

$$d^j_{\lambda\mu}(\theta)\simeq J_n((J+1/2)\omega)\qquad\qquad n=|\mu-\lambda|.$$

Substituting in the Jacob-Wick Expansion and approximating the sum by an integral we obtain

$$\langle\lambda_c\lambda_d|M|\lambda_a\lambda_b\rangle_n\simeq\int_{J_0}^\infty xdx\langle\lambda_c\lambda_d|M(x)|\lambda_a\lambda_b\rangle_n J_n(\omega x).$$

Comparing this formula with the one obtained by using the approximate amplitudes M_n^a and using the integral formula above, we write

$$M_n^a = \frac{\theta}{qq'}[(x_{an}-\varepsilon^2\bar{x}_{an})\frac{\omega^n}{\varepsilon^2+\omega^2} + \omega^n\bar{x}_{an}]$$
$$= \frac{\theta}{qq'}[(x_{an}-\varepsilon^2\bar{x}_{an})\int_0^\infty xdxJ_n(\omega x)K_n(\varepsilon x)+\omega^n\bar{x}_{an}].$$

Adding DW(X) under the integral in M is essentially the correct procedure for adding the distorted wave corrections.

It is possible to write the absorptive amplitude for a process in a way that explicitly separates the correction term from the Born exchange contribution. We begin with the Sopkovich formula for absorptive corrections:

$$\langle\lambda_c\lambda_d|T_j^A|\lambda_a\lambda_b\rangle = e^{i\delta_j^F}\langle\lambda_c\lambda_d|T_j^B|\lambda_a\lambda_b\rangle e^{i\delta_j^I}$$
$$= \sqrt{S_j^F}\text{----------}\sqrt{S_i^I}.$$

Writing $S_j=1+2iNT_j$ where N=normalization and energy momentum conservation, we readily obtain

$$\langle\lambda_c\lambda_d|T^A|\lambda_a\lambda_b\rangle_n = \langle\lambda_c\lambda_d|T^B|\lambda_a\lambda_b\rangle$$
$$+iN_j^F\sum_{\lambda_1\lambda_2}(2_j+1)d^j_{\lambda\mu}(\theta)\langle\lambda_c\lambda_d|T^F,|\lambda_1\lambda_2\rangle\langle\lambda_1\lambda_2|T_j^B|\lambda_a\lambda_b\rangle$$
$$+iN_j^I\sum_{\lambda_1\lambda_2}(2_j+1)d^j_{\lambda\mu}(\theta)\langle\lambda_c\lambda_d|T_j^B|\lambda_1\lambda_2\rangle\langle\lambda_1\lambda_2|T_j^I|\lambda_a\lambda_b\rangle$$
$$-N_i^IN^F\Sigma(2_j+1)d^j_{\lambda\mu}(\theta)\langle\lambda_c\lambda_d|T_j^F|\lambda_1\lambda_2|T_j^B|\lambda_3\lambda_4\rangle\langle\lambda_3\lambda_4|T_j^I|\lambda_a\lambda_b\rangle+\ldots$$

where the Jacob-Wick expansion has been used to obtain the full amplitude. If we approximate the initial and final state elastic scattering amplitudes by spin-independent functions we recover our simpler, less general, formula

$$\langle\lambda_c\lambda_d|T^A|\lambda_a\lambda_b\rangle = \sum_j (2_j+1)\,[1+iT_j^F N^F + iT_j^I N^I - T_j^F T_j^I N^F N^I + \ldots]$$

$$\langle\lambda_c\lambda_d|T_j^B|\lambda_a\lambda_b\rangle d^j_{\lambda\mu}(\theta)$$

$$= \sum_j (2_j+1) DW_j \langle\lambda_c\lambda_d|T_j^B|\lambda_a\lambda_b\rangle d^j_{\lambda\mu}(\theta).$$

The general formula is useful as a starting point for more sophisticated calculations, eg. spin-flip in the elastic scattering which would allow one to take into account the non-zero polarization found in many elastic collisions, and to see more clearly the effects of absorptive corrections on the exchange amplitude. In practice, calculations using this form require large quantities of computer time.

FORM FACTORS

One of the first ideas for improvement of the Born Term Model was to replace the simple point vertex functions and the propagator by functions which incorporate higher order effects. The existence of such effects was used to justify replacement of the Born amplitude B by BF, where F is some phenomenological function depending on t and the masses and as few arbitrary constants as possible. If one chooses such a function and obtains a best fit to the data at some incident energy and then uses this function to calculate at other energies, he hopes to succeed in comparing with experiment. If success does come, one has a very simple method of calculating.

J. D. Jackson and H. Pilkuhn[5] used an exponential form factor $e^{\lambda t}$ to improve the angular distribution in fits to KN→K*N and K*N* over that obtained from simple vector meson exchange. Later we will see that such a form factor works well for πN inelastic collisions dominated by vector meson exchange, but that another form factor F(s) is necessary to fit the energy dependence.

Form factors are also able to improve on the Born model for reactions dominated by the exchange of pseudoscalar particles. Amaldi and Selleri,[6] two of the early investigators of peripheral collisions, were successful in fitting the data on $\pi p \rightarrow \rho p$ with the function

$$F(t)=\frac{0.72}{1+(M_\pi^2-t)/4.73M_\pi^2}+\frac{0.28}{1+[(M_\pi^2-t)/32M_\pi^2]^2}$$

A REGGE MODEL

Another approach based on an idea first suggested by Gell-mann, Frautschi, and Zacharisen,[7] draws on the Regge Model of high energy scattering. One starts with the t-channel process, writing down a partial wave expansion for the amplitude. Assuming a resonance in a partial wave one performs an analytic continuation via the Sommerfield-Watson transform to the s channel. This amplitude, the contribution to the s channel amplitude due to the virtual exchange of the t-channel resonance, is used to calculate cross-sections. One obtains a one-meson exchange model in a different way; the exchanged particle has a spin $\alpha(t)$. One can show that the characteristic propagator form $\frac{1}{t-M_e^2}$ is contained in the amplitude.

Many authors have done calculations based on this model.[8] The idea is to replace the factor $\frac{p}{t-M_e^2}$ in the one-meson exchange amplitude, the one obtained field theoretically and not the one crossed from t channel by a phenomenological function of Regge form:

$$\frac{F(t)}{t-M_e^2} \; K \frac{(2\alpha(t)+1)\,(1+\tau e^{-i\pi\alpha(t)})}{2\sin\pi\alpha_\pi} \left[\frac{s-u}{4q_t q_t'}\right]^{\alpha(t)} \left[\frac{q_t q_t'}{M_a \sqrt{M_b M_d}}\right]^{\alpha(t)}$$

The trajectory $\alpha(t)$ is determined experimentally. This is done for each exchanged particle. The extra factors have been introduced to make the formula dimensionally simple. The basis for this replacement is that had we started with the t-channel amplitude $T_t(s,t)=k\sum_\ell(2\ell+1)T_\ell(\varepsilon_t)P_\ell(\cos\theta_t)$, assumed dominance of a resonance of spin ℓ, performed the Sommerfield-Watson transform and continued to the s channel we would not get a factor $\frac{1}{M_e^2-t}$. Instead we would have obtained something like

$$\frac{\delta(t)}{\sin\pi\alpha(t)}\left(\frac{s}{s_0}\right)^{\alpha(t)} \qquad \text{where } J=\mathrm{Re}\,\alpha(M_e^2),$$

where (t) will have the behavior $\frac{1}{t-M_e^2}$, provided it is not destroyed by other factors in δ. This does happen occasionally. Starting with the Regge Form

$$(2\pi+1)\left(\frac{P_\alpha(-x_t)+P_\alpha(x_t)}{2\sin\pi\alpha}\right)\left(\frac{q_tq_t'}{M_a\sqrt{M}\,M_d}\right)^{\alpha(t)}B$$

where q_t, q_t' are initial, final cm momenta for t-channel; using

$$x_t=\cos\theta_t=\frac{s-u}{4q_tq_t'} \quad \delta>>t \quad \frac{s-1/2(M_a^2+M_b^2+M_c^2+M_d^2)}{2q_tq_t'}$$

and

$$P_\alpha(\chi_t)\sim\frac{\Gamma(\alpha+1/2)2^\alpha}{\sqrt{\pi}\Gamma(\alpha+1)}\chi_t^{\alpha(t)}=C\chi_t^{\alpha(t)} \quad P_\alpha(-x_t)=te^{-i\pi\alpha}P_\alpha(x_t)$$

we write

$$\bar{B}(2\alpha(t)+1)\frac{1+\tau e^{-i\pi\alpha(t)}}{2\sin\pi\alpha(t)}\chi_t^\alpha\left[\frac{q_tq_t'}{M_a\sqrt{M_b}M_d}\right]^{\alpha(t)} \quad \text{where have put}$$

$cB=\bar{B}$ and τ is the signature of the exchanged trajectory.

$\bar{B}$ is determined by requiring this expression to coincide with the field theory propagator at the pole $t=M_e^2$

$$\lim_{t\to M_e^2}[\bar{B}(2\alpha(t)+1)\ \frac{1+te^{-i\pi\alpha(t)}}{2\ \sin\pi\alpha(t)}\ \chi_t^{\alpha(t)}[\,]^{\alpha(t)}=\frac{1}{t-M_e^2}\ .$$

Near the pole (at t_0)

$$\alpha(t)\approx\alpha(t_0)+\alpha'(t_0)(t-t_0)$$

$$\sin\pi\alpha(t)\ \approx\ \sin\pi\alpha(t_0)+\pi\alpha'(t_0)\cos\pi\alpha(t_0)(t-t_0)$$

$$\approx\ \sin\pi j+\pi\alpha'(t_0)\cos\pi j(t-t_0)\approx\pi\alpha'(t_0)(t-t_0)\cos\pi j$$

$$\approx\ \pi\alpha'(t_0)(t-t_0)(-)^j$$

=>

$$\lim_{t\to t_0}[\bar{B}(2j+1)\frac{1+\tau(-)^j}{2(-)^j\pi\alpha'(t_0)(t-t_0)}\ \chi_t^j[\,]^j\ =\ \frac{1}{t-t_0}]$$

from which we readily obtain

$$\bar{B}\ =\ 2\pi\alpha'(t_0)\chi_t^{-j}/[(\tau+(-)^j)(2_j+1)]$$

$$=\ \frac{2\pi\alpha'(t_0)}{(2_j+1)[\tau+(-)^j]}\{\ \frac{s-1/2(M_a^2+M_b^2+M_c^2+M_d^2)}{2M_a\sqrt{M_b}M_d}\}^{-j}$$

Example:

For J=1 exchange the propagator is replaced by

$$R(t)=\bar{B}(2\alpha(t)+1)\frac{i-e^{-i\pi\alpha(t)}}{2\sin\pi\alpha(t)}\{\ \frac{s-1/2(M_a^2+M_b^2+M_c^2+M_d^2)}{2M_a\sqrt{M_b}M_d}\}^{\alpha(t)}$$

where $\bar{B}$ is given by

$$\bar{B}=\ -\frac{\pi}{3}\alpha'_{J=1}(t_0)\{\frac{s-1/2(M_a^2+M_b^2+M_c^2+M_d^2)}{2M_a\sqrt{M_b}M_d}\}^{\alpha(t)}$$

The procedure is to calculate the cross-section and density matrix elements with this form for the propagotor using the experimentally determined Regge trajectory appropriate to the exchanged state. Since the Regge model is known to give the correct asymptotic energy dependence for cross-sections one hopes that this phenomenological ansatz based on the Regge idea will show similar socially acceptable behavior when it comes to energy dependence. The problem of correct energy dependence is one of the chief difficulties of the other methods of calculating peripheral reactions. As a derivation of one-particle-exchange via the Regge approach makes clear, the energy dependence is intimately connected with the spin of the exchanged quanta. In the Regge approach, exchange of a spin j does not lead to amplitudes which go as s^j but as $s^{\alpha_j(t)}$ where $\alpha_j(t)$ is the trajectory of the exchanged quanta.

We might wonder why the field theoretic t-channel amplitude is not used and explicitly continued to the s-channel rather than making this propagator replacement. Such calculations are being done and they are more complicated than the replacement procedure. Starting with the t-channel exchange amplitude, the kinematical singularities introduced by spin are explicitly removed and the amplitude is continued analytically to the physical s-channel region.

Again, the residues are determined by requiring equality with the Born term at the pole. As an example of such calculations, the reader is referred to the recent work of Griffiths and Jabbur[9] on N*3 production, in KN collisions. Recent calculations on np charge exchange combining the absorption model with a consistent treatment of spin in the Regge model will be outlined later in this paper.

ONE-MESON-EXCHANGE CALCULATIONS AND COMPARISON WITH EXPERIMENTS

Most of the basic approaches to theoretical analysis of peripheral collisions have been discussed. To familiarize the reader with the general picture before describing present attempts to find improvements to OME models, consider two reactions. One, $\pi N \to \rho N$, is dominated by pseudoscalar meson exchange, the other, $\pi n \to \omega p$, by vector meson exchange. We discuss them in terms of the models just outlined. This discussion will be qualitative. The figures show general s and t behavior only. Notation and conventions are detailed in Appendix I.

The first of these reactions has been studied by many high energy theorists [3] and summarizes the successes of the models. This is both good and bad. It is good that everyone can invent a model, but bad because there is no resultant discrimination among ideas. The second reaction has been chosen because none of the models already discussed can explain all of the data. Some models give correct angular distributions and others handle the energy-dependence.

Figure 6 shows $\frac{d\sigma}{d\Omega}$ vs t for each of the reactions on a linear scale of arbitrary normalization.

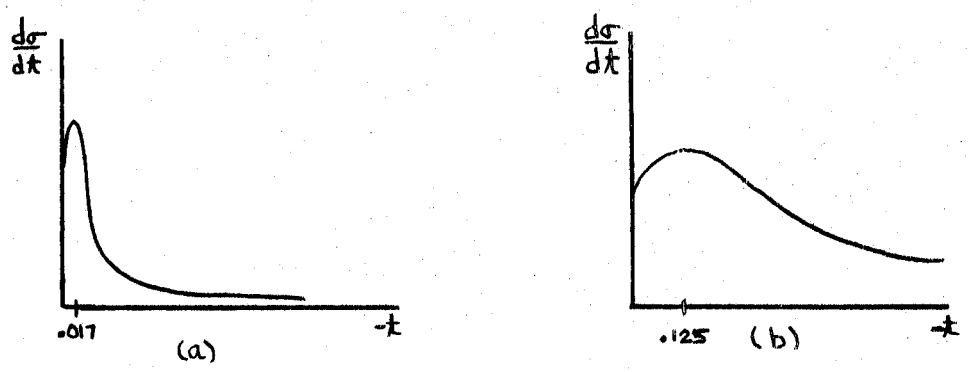

Figure 6. Qualitative sketches of the t-angular distributions for (a) $\pi p \to \rho p$ at 4.0 GeV/c and (b) $\pi n \to \omega p$ at 3.25 GeV/c.

Notice the peaking, particularly strong for $\pi p \to \rho p$, in the forward direction. This peaking is characteristic of peripheral processes. The angular distribution for $\pi^+ n \to \omega p$, dominated by ρ exchange, is less peripheral than the π-exchange reaction, as is to be expected since m_ρ is much larger than m_π. In each case the total cross-section drops quickly with increasing energy as indicated in Figure 7.

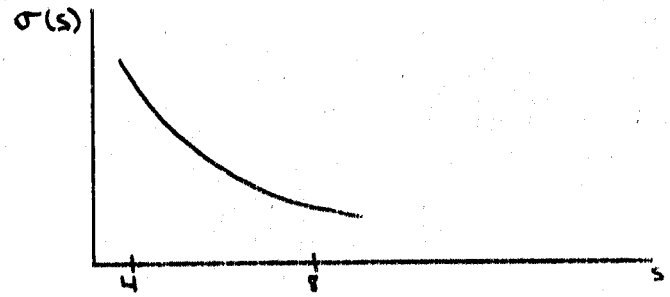

Figure 7. Sketch of s-dependence of the total cross-section in a quasi two body high energy scattering involving quantum number exchange.

Data on the production density matrix are meager. Because of invariance principles, there are only three elements of interest and they are the same ones for each reaction: $\rho_{00}, \rho_{10}, \rho_{1,-1}$. The element ρ_{10} is complex but we need only the real part for the decay distributions $W(\cos\alpha)$ and $W(\beta)$. For $\pi p \to \rho p$ at 4.0 GeV/c the available data are $\langle\rho_{00}\rangle = 0.53\pm0.12$, $\langle\rho_{1,-1}\rangle = 0.16\pm0.10$, $\langle\rho_{10}\rangle = -0.06\pm0.05$. Similarly, for $\pi^+ n(\rho)\omega p$ at 3.25 GeV/c Jackson gives $\langle\rho_{00}\rangle = 0.5$ and at 1.7 GeV/c he gives $\langle\rho_{00}\rangle = 0.6\pm0.12$, $\langle\rho_{1,-1}\rangle = 0.0\pm0.712$, $\langle\rho_{10}\rangle = -0.06\pm0.08$. In both cases the average is over $\cos\theta$ from 1.0 to about 0.80. This data is not very limiting to a model, but we shall see that it does tell us something.

The Born Term Model (BTM)

If we superimpose theoretical curves for $\frac{d\sigma}{dt}$ on the experimental data as indicated in Figure 8 we see immediately that the BTM is just not good enough. The cross-sections are too large and not nearly peripheral enough. It should be noted that the vector-meson-baryon coupling involves an arbitrary factor. There are two coupling constants, the vector coupling G_V and the tensor G_T. Even if one uses some symmetry scheme to fix G_V, he must look elsewhere to get G_{T/G_V}. Jackson gives $^{G_T/G_V} = 3.7$ inferred from T=1 electromagnetic form factors.

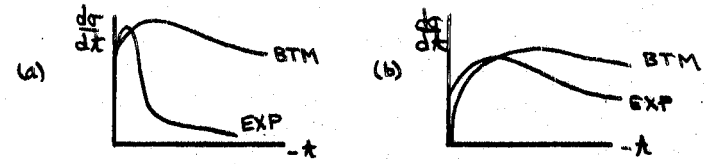

Figure 8. Comparison sketches of the BTM and experimental (EXP) for (a) $\pi p \to \rho p$ and (b) $\pi n \to \omega p$.

Comparison of theoretical and experimental total cross-sections and density matrix elements is as unfavorable as for the angular distribution. The energy dependence is particularly bad for the vector meson exchange reaction. But it is of practical value to carry through an analysis to determine the BTM predictions for $\rho_{mm'}$. It is not necessary to do any calculating to get answers. For $\pi^- p(\pi)\rho^- p$, Figure 9 shows the $\pi\pi\rho$ vertex in the ρ rest frame.

Figure 9. The $\pi\pi\rho$-vertex in the ρ-meson rest frame.

This case was considered in the discussion of density matrix elements. The analysis was done in the rest frame of the ρ-meson and we concluded that the only non-vanishing element is ρ_{00} and using the normalization condition $Tr\rho = 1$ we obtained $\rho_{00}=1$. The data tell us that the BTM prediction is incorrect.

We ask if the fault is with the BTM or with the quantum we have assumed to be exchanged. To answer this we look at the decay angular distributions of the resonant

state, $W(\cos\alpha)$ and $W(\rho)$ and note that even though $\rho_{1,-1}$ and ρ_{10} are doubtless non-zero, they are extremely small, which is consistent with pseudoscalar exchange. The experimental W's, shown in Figure 10 support this conclusion.

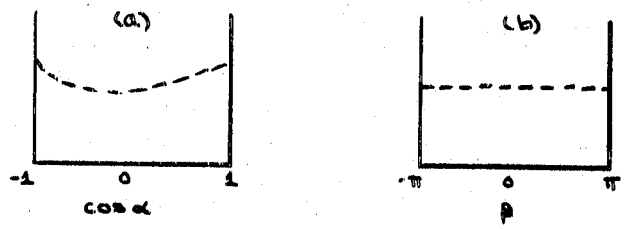

Figure 10. Sketches showing the experimental decay distributions for the decay $\rho\to\pi\pi$ in the reaction $\pi p\to\rho p\to\pi\pi p$ assuming 0 exchange (a) $W(\cos\alpha)$ (b) $W(\beta)$.

Additional support comes from the BTM distributions assuming vector meson exchange which is also allowed in this reaction. Figure 11 shows these distributions. (We will see how to obtain these distributions shortly). It is apparent that these distributions are not at all close to the experimental data. The conclusion is that the basic idea of pseudoscalar exchange dominance is a good one but that it is too simple; the BTM neglects too much.

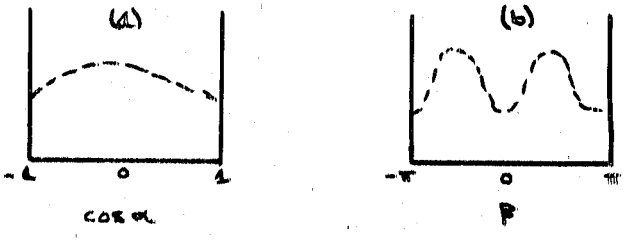

Figure 11. Sketches showing the experimental decay distributions for the decay $\rho\to\pi\pi$ in the reaction $\pi p\to\rho p\to\pi\pi p$ assuming 1 exchange (a) $W(\cos\alpha)$ (b) $W(\beta)$.

For $\pi^+ n \to \omega p$ the analysis procedes in the same manner as for 0^- exchange. In the rest frame of the ω, we have, from the angular momentum addition theorem that $0^- + J_e^p + L^{(-)^L} = 1^-$; $J_e = 1$ implies L=0, 1, or 2 and, since we are in the ω rest frame, $L_z = 0$. The conservation of parity in strong interactions tells us that $(-)P_e(-)^L = (-)$ or L must be odd, since $P_e = -1$. Therefore L=1. Conservation of the z-component of J tells us that $J_{ez} = 0, \pm 1$. So we must have $|1m\rangle_e$ coupled to $|10\rangle_L$ to produce $|1m\rangle_\omega$. Again by the rules for adding momenta we see that the state $|1m\rangle_e |10\rangle_L$ contains only $|1\pm1\rangle_\omega$ ie. the $m_\omega = 0$ state is not produced. Therefore we can conclude that $\rho_{mo} = \rho_{om} = 0$. Substituting in the decay angular distribution formulas we obtain

$$W(\cos\alpha, \beta) = 3/4\pi (1/2 - \rho_{1,-1}\cos 2\beta)\sin^2\alpha$$

or

$$W(\cos\alpha) = 3/4 \sin^2\alpha \qquad W(\beta) = 1/4\pi (1 + 2\rho_{1,-1}) - 4\rho_{1,-1}\cos^2\beta).$$

(These formulas are valid for ω decay even though it is a 3π resonance if the angles are redefined such that α is the angle between the incident π^+ and the normal to the $\pi^-\pi^\circ$ decay pion plane; β is then the corresponding azimuthal angle).

We see immediately that for vector meson production in PB collisions the decay angular distributions are distinctly different for pseudoscalar and vector exchange dominance. (Actually the above analysis is valid for an exchanged state with $P_e=(-)^{J_e}$, $J_e>1$; these are called natural parity states. For unnatural parity, $P_e=(-)^{J_e+1}$ we get no restrictions).

Figure 12 shows the experimental W's for $\pi^+ n \to \omega p$. It is clear that the evidence is strong for the exchange of a natural parity state. The simplest possible exchange candidate is the ρ-meson, a member of the 1^- octet.

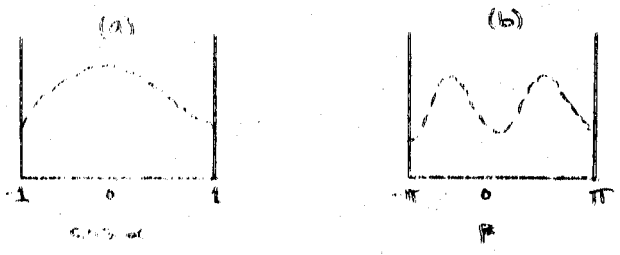

Figure 12. Sketches of the experimental decay distributions of ω in the reaction $\pi n \to \omega p$ (a) $W(\cos\alpha)$ (b) $W(\beta)$.

Multiplicative Form Factors and Reggeized Propagators

Both of these approaches involve replacing the exchange amplitude M^{EX} by $M^{EX}F(s,t)$, where $F(s,t)$ is a suitable function with as few aribtrary parameters as possible. Figure 13a shows the effect of the Amaldi-Selleri form factor on the π-exchange BTM cross-section for $\pi p \to \rho^- p$. The effect is to damp the amplitude at

larger values of t. This model compares favorably with experiment for incident pion momenta from 3.0 to 8.0 or 9.0 GeV/c in the lab. The same information is given in Figure 13 b for the Regge propagator model.

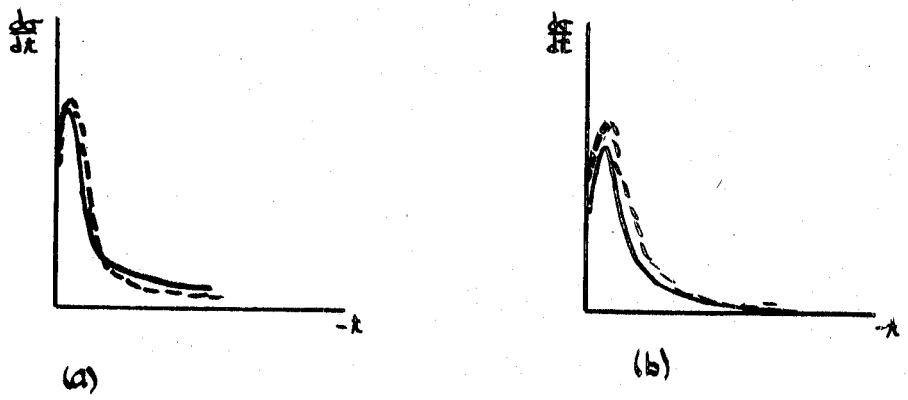

Figure 13. Comparison sketches of (a) BTMF and (b) BTMR with experiment of the reaction $\pi p \to \rho p$. The dashed curves are the experimental results. $\frac{d\sigma}{dt}(t=0)$ is matched to the theoretical calculation at t=0.

One can see that the results are favorable. Again, the effect of this modification is to damp the Born amplitude at larger values of t, which is the desired effect. There is some arbitrariness in the pion trajectory; since it is difficult to isolate experimentally one determines the form from general principles.

For vector exchange reactions, Jackson and Pilkuhn improved the BTM angular distributions with an exponential form $E(0)e^{-\lambda t}$ (usually normalize form factors to 1 at the exchange pole: $F(t=m_e^2)=1$; $E(0)=1e^{-\lambda m_e^2}$).

Figure 14a shows the effect of such a factor with $\lambda=2.5(\text{GeV/c})^{-2}$ on the $\pi^+n\to\omega p$ reaction. We see an improvement in the angular distribution. There is, of course, not any improvement in the energy dependence. We could always add a factor S^{-n} and adjust n for a best fit. The Regge propagator result is shown in 14b. The trajectory used in the calculation is $\alpha_\rho(t)=.57+1.08t$; the parameters are from experiment. The energy dependence also considerably improved.

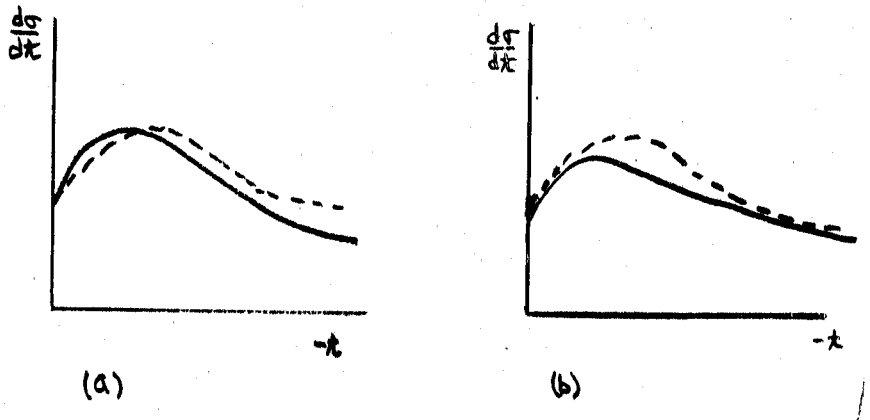

Figure 14. Comparison sketches of (a) BTMF and (b) BTMR with experiment for the reaction $\pi n\to\omega p$. The dashed curves are the experimental results. $\frac{d\sigma}{dt}(t=0)$ is matched to the theoretical calculation at t=0. Theory and experiment are on the same scale.

Neither of these modifications to the BTM affect the density matrix predictions; no spin-independent modifications can do so. To see this we look closely at the definition of $\rho_{mm'}$, assuming a resonant state d:

$$\rho_{mm'} = N\Sigma\langle\lambda_c m|M|\lambda_a\lambda_b\rangle\langle\lambda_c m'|M|\lambda_a\lambda_b\rangle^* \qquad Tr\rho=1$$

where $\langle|M|\rangle$ are the production helicity amplitudes.

If M denotes the BTM amplitude and F a function, <u>independent of spin</u>, then the form factor modified or reggeized propagator amplitude is MF. Since F factors we have

$$\rho = N|F|^2\Sigma\langle|M|\rangle\langle|M|\rangle^* = N|F|^2A^{-1}$$

and we see immediately that $Tr\rho = 1$ gives $N=A|F|^{-2}$ and $\rho_{mm'}$ is unaffected.

Absorptive Corrections

By the same kind of argument, it is apparent that the absorptive corrections <u>will</u> modify the density matrix elements because the effective function F is different for each spin amplitude. However, since absorption usually damps down contributions to the lower partial waves much more than the high ones for each amplitude one expects the modifications to $\rho^{BTM}_{mm'}$ to be small for most of the elements--exactly the experimental situation.

For the π-exchange reaction it is difficult to distinguish between the absorptive and Regge calculations. The results are not identical but they are close for scale and angular distribution. The density matrix prediction of the absorption model is good, while the BTMR calculation gives the same prediction as the BTM. The situation is somewhat different for the ρ-exchange reaction, $\pi^+ n \to \omega p$. Again the absorptive model does well with angular distribution and density matrix elements but the absolute magnitude of the total cross-section prediction is too high. In this regard, the Regge propagator form does much better. Because the meager data we cannot say just how much better; it is possible that the prediction is low. As in the ρ-case, this Regge model gives no improvement in the production density matrix prediction over that of the BTM.

The absorptive corrections for these calculations were obtained from phenomenological fits to experiment according to the prescription of Jackson and Gottfried[4] (1964). This approach is quite successful and is used by most everyone doing absorptive calculations. The idea is too obtain from the latest experimental data a best fit to the elastic scattering amplitude and invert it to obtain the elastic phase shift which is then used to correct the inelastic amplitude.

Recall the DWBA formula for the elastic scattering amplitude:

$$f_{EL} = -\lambda\int d\underline{r}\; e^{-i\underline{q}'\cdot\underline{r}}V(\underline{r})\chi(\underline{r})$$

Substituting the high energy approximate expression for $\chi(\underline{u})$ we obtain

$$f_{EL} = -\lambda\int d\underline{r}\; e^{-i\underline{q}'\cdot\underline{r}}V(\underline{r})e^{i\underline{q}\cdot\underline{r}-i\frac{\lambda}{q}\int_{-\infty}^{z}dz'V(b,z')}$$

$$= -iq\int bdbd\theta dz\frac{d}{dz}\; e^{-i\frac{\lambda}{q}\int_{-\infty}^{}dz'V(b,z')}e^{i\underline{\Delta}\cdot\underline{b}} \qquad \Delta=q-q'$$

(for $\theta<<1$ $\underline{\Delta}\;\underline{q} = \underline{2}q$ so $\underline{\Delta}\cdot\underline{r}\tilde{}\;\underline{\Delta}\cdot\underline{b}$)

The integral over z gives $e^{-i\lambda/q\int_{-\infty}^{}dz'V(b,z')}-1=$ $e^{i\chi(b)}-1$. After the integration over θ we obtain the Glauber formula.

$$f_{EL} = -iq\int bdbJ_0(\,b)[e^{i\chi(b)}-1]$$

using $\int bdbj_n(\Delta b)J_n(\Delta' b) = \frac{1}{\Delta}\delta(\Delta-\Delta')$

we obtain

$$e^{i\chi(b)} = 1+\frac{i}{q}\int\Delta d\Delta J_0(\Delta b)f_{EL}(\Delta)$$

The standard parameterization of the experimental data on elastic scattering is a Gaussian distribution in Δ:

$$f_{EL} = \frac{i\sigma_T q}{4\pi}\; e^{-c\Delta^2} \qquad C = \frac{\sigma_T}{\gamma\pi c} \qquad \gamma = \frac{1}{4c}$$

$$= \frac{iC\gamma q}{2}\; e^{-\Delta^2/4\gamma}$$

Substitution in the Glauber formula readily gives

$$e^{i\chi(b)} = 1-Ce^{-\gamma J^2/q^2}$$

The parameters C,γ are directly related to experimental quantities. Usually they are assumed independent of energy. One fits them to the available data at one incident energy and calculates the inelastic cross-sections over a range of energies and compares with experiment. The results are quite good for many reactions, but the very best fits to the data require energy dependent C and γ.

A very similar record of successes and failure appears in other πN channel reactions and in KN and NN reactions. The success or failure of a model depends more on the tensor character of the exchanged quanta than on the nature of the final state (eg. one resonance, two resonances, etc.--). To summarize:

1. The Born Term Model (BTM) while exhibiting some nice features is inadequate. Looking at the experimental data we intuitively conclude that we should try to modify it in some way rather than abandon it alltogether. One makes this decision because one-particle exchange is relatively simple to calculate. Also, the density matrix data show quite well the effects expected from one-particle exchange.

2. Simple phenomenological form factors F(t) can provide agreement with the production angular distribution data over a respectable range of energies--particularly for ρ-exchange. Sometimes (ρ-exchange) one also gets good $\sigma_T(s)$ vs. s; for some reactions an additional factor F(s) is necessary. No improvement in density matrix elements is obtained.

3. The Regge form of the propagator works well for production angular distributions and does much better on energy dependence than the BTM, but fails on density matrix elements. More sophisticated Regge calculations can give $\rho_{mm'}$ predictions. Basically this approach is quite like using a form factor.

4. The absorptive model performs extremely well whenever reactions go via pseudoscalar exchange. It gives good $\sigma_T(s)$ vs. s, good $\frac{d\sigma}{dt}$ vs. t and usually good absolute magnitude. Also, predictions on $\rho_{mm'}$ are good. Whenever V-exchange dominates, the angular shape is good and density matrix predictions are acceptable, but absolute magnitude of cross-sections is too large and the energy dependence prediction incorrect.

ANOTHER APPROACH TO ABSORPTIVE CORRECTIONS

One can try to be more ambitious in applying absorptive corrections to inelastic BTM amplitudes. Instead of purely phenomenological fits to the elastic scattering data, one can construct models for the elastic amplitude based on physical ideas, hopefully containing as few parameters as possible and use them to generate absorptive corrections. If the model is good we expect a fine fit to the elastic scattering and to the inelastic processes with the same values for the parameters. We consider one such model.

Recently S. Frautschi and B. Margolis[10] proposed a model of high energy elastic scattering based on the identification of the Born term with Regge exchange. The t-channel Regge exchange is assumed to generate the s-channel potential rather than the amplitude. They start with the Born approximation to Glauber's formula:

$$f^B_{EL}(\Delta,q) = -\frac{iq}{2\pi}\int d^2b 2i\delta(b) e^{ib\cdot q}$$

The physics enters here. f^B_{EL} is equated to the leading Regge trajectory pole contribution

$$A_{pole}=ce^{\mu\alpha(t)}$$

$\mu=\ln\frac{s}{s_0}-i\pi/2$, signature is neglected, $\alpha(t)$ is the Pomeranchuk trajectory $\alpha(t)\simeq\alpha(t_0)+\alpha'(t-t_0)$

$$A_p=ce^{\mu\alpha(t)}=-\frac{iq}{2\pi}\int d^2b 2i\delta(b)e^{ib\cdot q}$$

Frautschi and Margolis then solve for $\delta(b)$ and sum the Born Series to obtain an expression for the elastic amplitude, an amplitude consisting of the pole term plus a series of multiple scattering terms which can be likened to Regge cuts. The one free parameter (the slope of the Pomeranchuk is obtained elsewhere) is fit to experiment at some incident energy and calculations are compared with experiment over a range of energies with much success.

This model can be used to generate absorptive corrections, which can be applied to inelastic processes in the spirit of the Jackson-Gottfried approach. Inverting the above equation we have

$$2i\delta(b) = -\frac{\xi}{\mu}e^{-b^2/4\alpha'\mu},$$

where we have assumed

$$\alpha_p(t)=1+\alpha' t.$$

Using this expression we obtain the corresponding absorptive correction function

$$e^{i\chi(b)}=e^{2i\delta(b)}=e^{-\xi/\mu}e^{-b^2/4\alpha'\mu}$$

Notice that

$$|e^{i\chi(b)}|\to 1 \quad \text{as } s\to\infty.$$

This absorption function has several features noticably different from the Jackson-Gottfried approach.

1. The correction is a complex function. We can expect the density matrix elements to be slightly different.

2. The correction is energy dependent and leads to a decrease in the amount of absorption as the energy increases. The effect is to soften the s-dependence of the BTM exchange.

We have compared this method of generating absorptive corrections with the curve fit approach for the reaction $pp \to n\Delta_{3/2}^{++}$. This reaction was chosen since Frautschi and Margolis have fit the parameter (ξ) in their hadron scattering model for p elastic scattering. As is usual, approximate equality of the absorptive correction function in the incident and final channel has been assumed in the absence of definitive NN* elastic scattering data.

Recall that the procedure is to replace the appropriate BTM partial wave amplitude M^j with

$\langle \lambda_c \lambda_d | M^j | \lambda_a \lambda_b \rangle DW_j$ $\qquad$ λ_i=helicity of i^{th} particle

The Jackson-Gottfried correction function has been parameterized as

$$(DW_j)^2 = [1 - c_+ e^{-\gamma_+^2 j^2/q_+^2}][1 - c_- e^{-\gamma_-^2 j^2/q_-^2}]$$

$\pm$ refer to incident and final channels, respectively.

The parameters $C\pm,\gamma\pm$ are derived from elastic pp scattering data to be:

$$C_{\pm}=1 \qquad \gamma_{+}=.24 \text{ GeV/c}$$

$$\gamma_{-}=.10 \text{ GeV/c}$$

In the model based approach, the absorptive function used is

$$(DW_j)^2 = \exp(-\frac{\xi_+}{\mu} e^{-J^2/4\alpha'\mu q_+^2}) \exp(-\frac{\xi_-}{\mu} e^{-J^2/4\alpha'\mu q_-^2})$$

We used the same value for the slope of the Pomeranchuk trajectory as Frautschi and Margolis: $\alpha'=0.82(\text{GeV/c})^{-2}$. Also, their fits to the elastic pp data at 20 GeV/c with this value of the slope and $s_0=1\text{GeV}^2$ yield $\xi=7$. Starting with $\xi_{\pm}=7$ this parameter was varied over a wide range to get a good fit to the $pp\rightarrow n\Delta^{++}_{3/2}$. Also, some calculations were done to determine the effect of different α' on the result.

The initial appeal of Frautschi's elastic scattering model for absorptive corrections is the logarithmic energy dependence which shows up in the expression for the phase shift. Absorptive model calculations a' la' Jackson-Gottfried at several energies show that the amount of absorption necessary to get a good phenomonological fit to the data decreases slowly with energy. It was hoped that the Frautschi parameterization of elastic scattering might allow for this decrease.

It is possible to get a good fit to $\frac{d\sigma}{dt}$, but at a particular energy there is trivial difference between the different approaches as shown in Figure 15. Differences in the predicted density matrix elements are easier to see--as a function of energy; the Frautschi model corrections give ρ_{mm}, which change more rapidly. Unfortunately there will not be enough good data until the summer, at which time comparison from 6-30 GeV/c should be possible.

There are other objections to this approach. From a phenomenological point of view it would be better to use the energy dependent corrections. But values of the absorptive parameters necessary to fit the inelastic data do not provide a satisfactory fit to the elastic scattering. Figure 16 compares a theoretical curve of the Frautschi model, using the parameters that provide a best fit to $pp \rightarrow n\Delta$ with the elastic scattering. It is not clear that the model is internally consistent. Sums of t-channel exchange diagrams can show a Regge behavior; the Frautschi model probably "double counts" contributions to the amplitude. Also, one can show that resonance behavior at low energy can be deduced from a Regge amplitude at high energy. Resonance is a property of amplitudes not potentials. The Frautschi model says that Regge exchange in one channel generates potentials in the crossed channel rather than amplitudes. This seems inconsistent with the other result.

We must conclude that the Frautschi model is probably not correct. It is possible to generate absorptive corrections containing a small energy dependence (any Regge model of elastic scattering can work) and improve, if only slightly, the fit to experiment. We are being drawn to simultaneous use of the Regge model and absorptive corrections. The only obstacle is the question of double counting--a question that <u>can</u> be answered in favor of combination of the models.

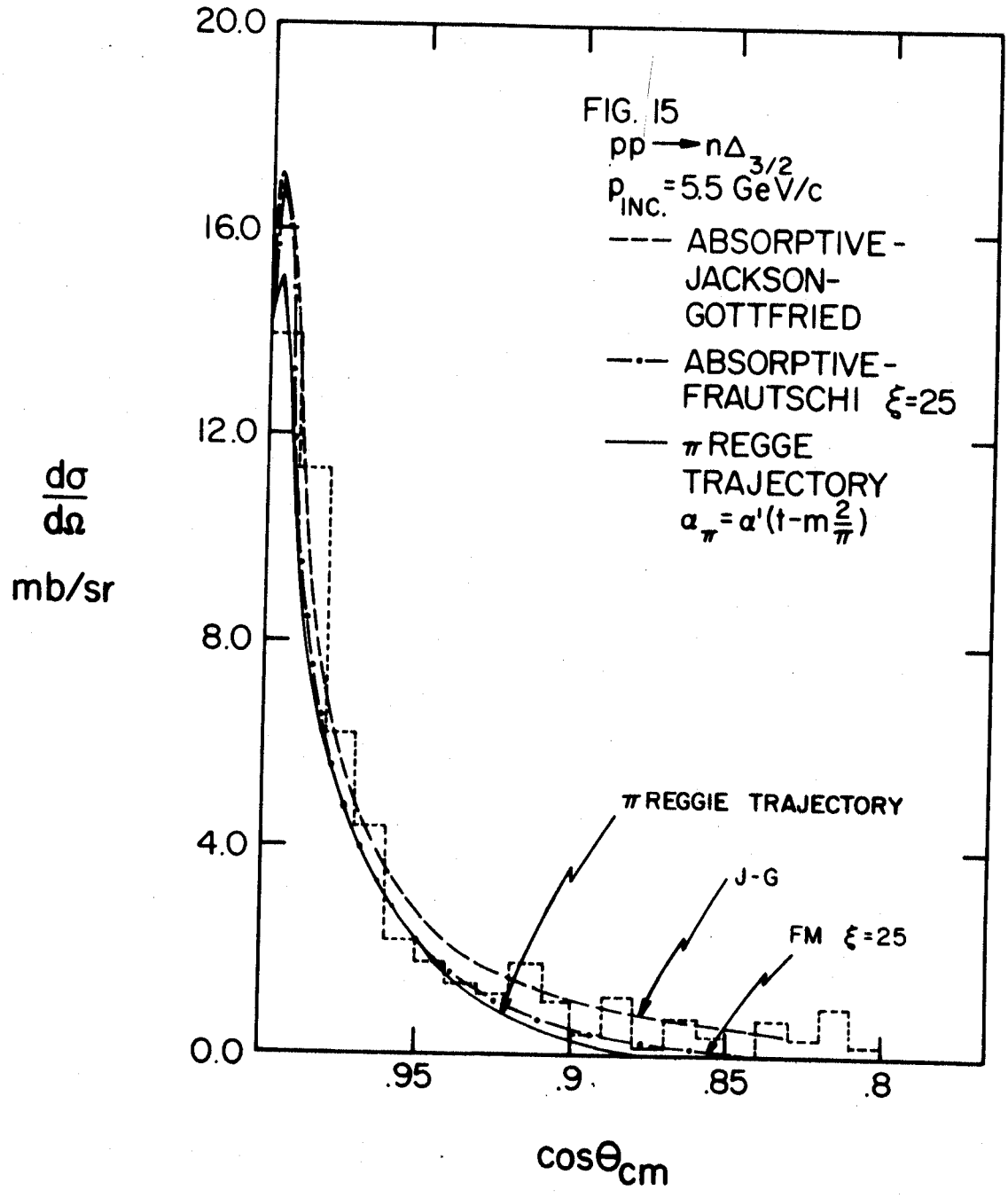

Figure 15. Comparison of theory and experiment for the reaction $pp \rightarrow n\Delta_{3/2}$.

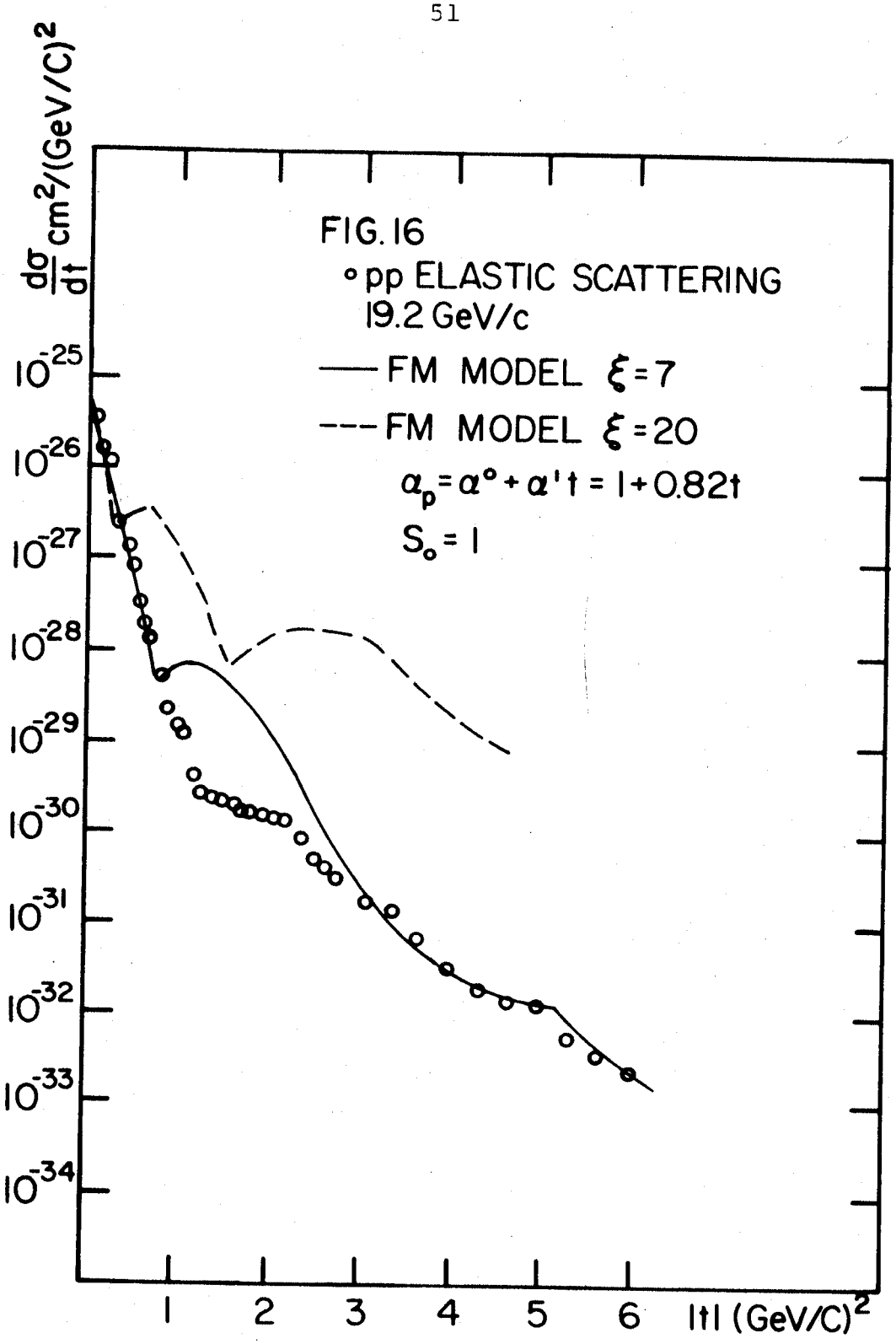

Figure 16. Comparison of pp elastic scattering with theory giving best fit to $pp \to n\Delta_{3/2}$.

OTHER MECHANISMS

With the successes and failures of one-meson-exchange in mind, we focus now on vector meson exchange and investigate improvements to OME models. As an example of a vector exchange dominated process we continue examination of $\pi n \to \omega p$.

Vertex Correction Mechanisms

The use of phenomenological form factors to improve simple OME was based on the assumption that other more complex diagrams contribute to the scattering amplitude, and that such factors (functions of t) improve the angular distribution over the BTM prediction for both pseudoscalar and vector meson exchange dominated reactions. We ask if it is possible to get a better clue as to the functional form of such factors by looking at other diagrams which can contribute. Figure 17 shows the diagrams for the BTM and lowest order corrections for $\pi^+ n \to \omega p$.

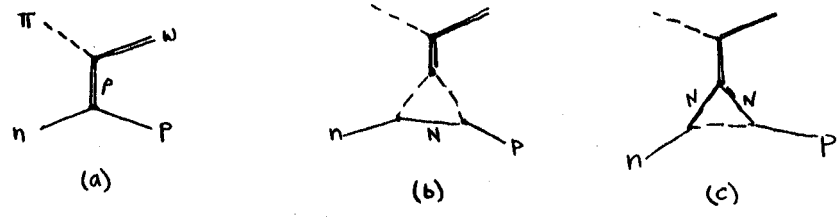

Figure 17. Diagrams showing (a) the BTM and (b)→(d) some vertex corrections to the NρN vertex for $\pi n \to \omega p$.

In addition there can be graphs where the virtual nucleons are replaced by nucleon resonances.

We concentrate on diagrams 17b as the next simple cases after the BTM. Using the Feynman rules for forming the S-matrix, we obtain the transition amplitude assuming this diagram to be the dominant contribution (detailed calculations can be found in Appendix III. We obtain

$$<\lambda_c\lambda_d|M|\lambda_b>_n = 2G_{NN}^2 g_{ppV}\frac{f_{vvp}}{M_c}\frac{1}{m^2-t}\varepsilon_{\mu\nu\rho\sigma}a\ e_\rho\varepsilon^*_\sigma(c,\lambda_c)$$
$$\bar{U}(d,\lambda_d)\gamma_5\Lambda_\mu\gamma_5 U(b,\lambda_b)$$

where

$$\gamma_5\Lambda_\mu\gamma_5=-2\Delta_{np}L_\mu^{(3)}(M_\rho)+2i\gamma_\lambda[L_{\lambda\mu}^{(3)}(M_\rho)-L_{\lambda\mu}^{(3)}(M_n)]$$

$$L_{\lambda\mu}^{(n)}(M)=\int ds\int\frac{d^4\ell}{(2\pi)^4}\frac{\ell_\lambda\ell_\mu}{[\ell^2-2\ell p_z+\Delta_z]^n} \qquad \Delta_{np}=M_n-M_p$$

All of the terms in Λ are finite, if one allows a liberal interpretation of the rules for manipulating infinite quantities. It is interesting to note that if we neglect the neutron-proton mass difference for internal lines the amplitude vanishes.

After very involved algebra, one obtains a compact expression for the helicity amplitudes

$$<\lambda_c\lambda_d|M|\lambda_b>_n = iK\frac{B^{\lambda c}\{\lambda_d,\lambda_b\}}{M_\rho^2-t}K[yz]$$

Here $\lambda_c,\lambda_d,\lambda_b$ refer to the helicity quantum number of the ω,ρ,n respectively. $\{\lambda_d,\lambda_b\}$ is shorthand for the spinor product $\bar{u}(p,\lambda_d)u(n,\lambda_b)$, K contains coupling constants and miscellaneous factors, and $B^{\lambda c}$ comes from the $\pi\rho\omega$ vertex. Consider first the energy dependence. Refering

to the BTM calculation one easily finds that the calculated $\frac{d\sigma}{d\Omega} \sim s^2$. We saw earlier that this result conflicts with the experimental evidence. Turning now to the vertex correction contribution, B and $\{\lambda_d, \lambda_b\}$ go as $s^{3/2}$ and s respectively ($k \sim s^0$). The energy dependence of K[YZ] is the only unknown. Should this factor, which comes from the closed loop in the diagram be independent of energy, we will obtain the same energy dependence of $\frac{d\sigma}{d\Omega}$ as the BTM. This will turn out to be the case. To see this we look more closely at the algebra. K[yz] can be expressed as a sum of three terms:

$$K[yz] = K_1[yz] + \frac{2M_\rho}{\Delta_{n\rho}} K_1'[y^2z^2] + 2K_1''[yz^2]$$

Where the first term comes out of $L^{(3)}(M_n)$ and the others from $2i\gamma_\lambda[L^{(3)}_{\mu\nu}(M_n) - L^{(3)}_{\mu\nu}(M)]$. Rewriting in terms of the fourth order Feynman parameter functions $F_i(x,z)$ defined in Appendix III we have

$$K_1[yz] = \frac{2}{(2\pi)^4} \int_0^1 dz\, F_3(1,z) M_n$$

$$K_1'[y^2z^2] = \frac{2}{(2\pi)^4} \int_0^1 dz\, z[F_5(1,z)M_n - F_5(1,z)M]$$

$$K_1''[yz^2] = \frac{2}{(2\pi)^4} \int_0^1 dz\, z\,[F_3(1,z)M_n - F_3(1,z)M]$$

This extra algebra proves very convenient; these functions $F_i(x,z)$ characteristic of fourth order diagrams in the πN channel.

Again refering to Appendix V , examination of the functions $F_i(x,z)$ shows clearly that all s-dependence vanishes at x=1: $F_i(1,z)$ are independent of s.

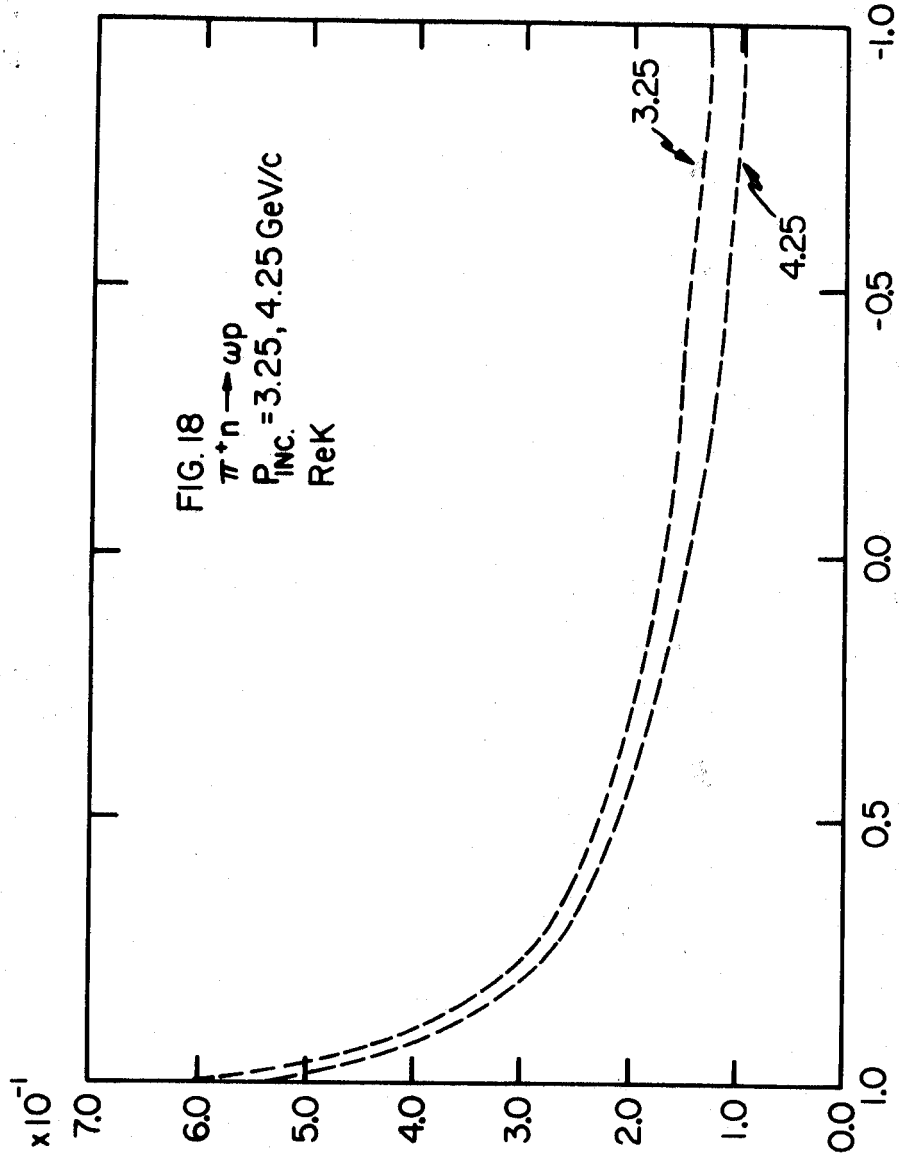

Figure 18. The real part of the structure function K[yz] over the physical range of t for the reaction $\pi n \rightarrow \omega p$.

Figure 18 shows ReK[yz] for several values of incident pion momentum over the physical range of t. (ImK 10^{-3}ReK) Notice the similarity in the curves for different energy and the forward peak. Since the scattering amplitude is proportional to $\omega^n K[yz]$ we can understand the peaking of $\frac{d\sigma}{d\Omega}$ at non-forward t. Assuming that these vertex correction type graphs are the dominant production mechanism for $\pi n \to \omega\rho$ the cross section was calculated, and is shown in Figure 19. The angular distribution is not bad and the absolute magnitude is more in line with experiment. Keep in mind that no absorptive corrections have been added. Addition of such corrections would shift the peak more toward the forward direction, but also would damp the absolute magnitude far to much. For comparison Figure 19 also shows the result of an absorptive BTM calculation at the same energy. Also, these graphs cannot improve the fit to the ω production density matrix elements; indeed the prediction is the same as the BTM.

Another approach would be to interpret these fourth order corrections in a strictly field theoretic sense as next order corrections to the BTM and assume

$$\langle \lambda_c \lambda_d | M | \lambda_b \rangle_n = \text{BTM} +$$

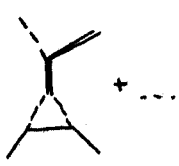

$+ \ldots$

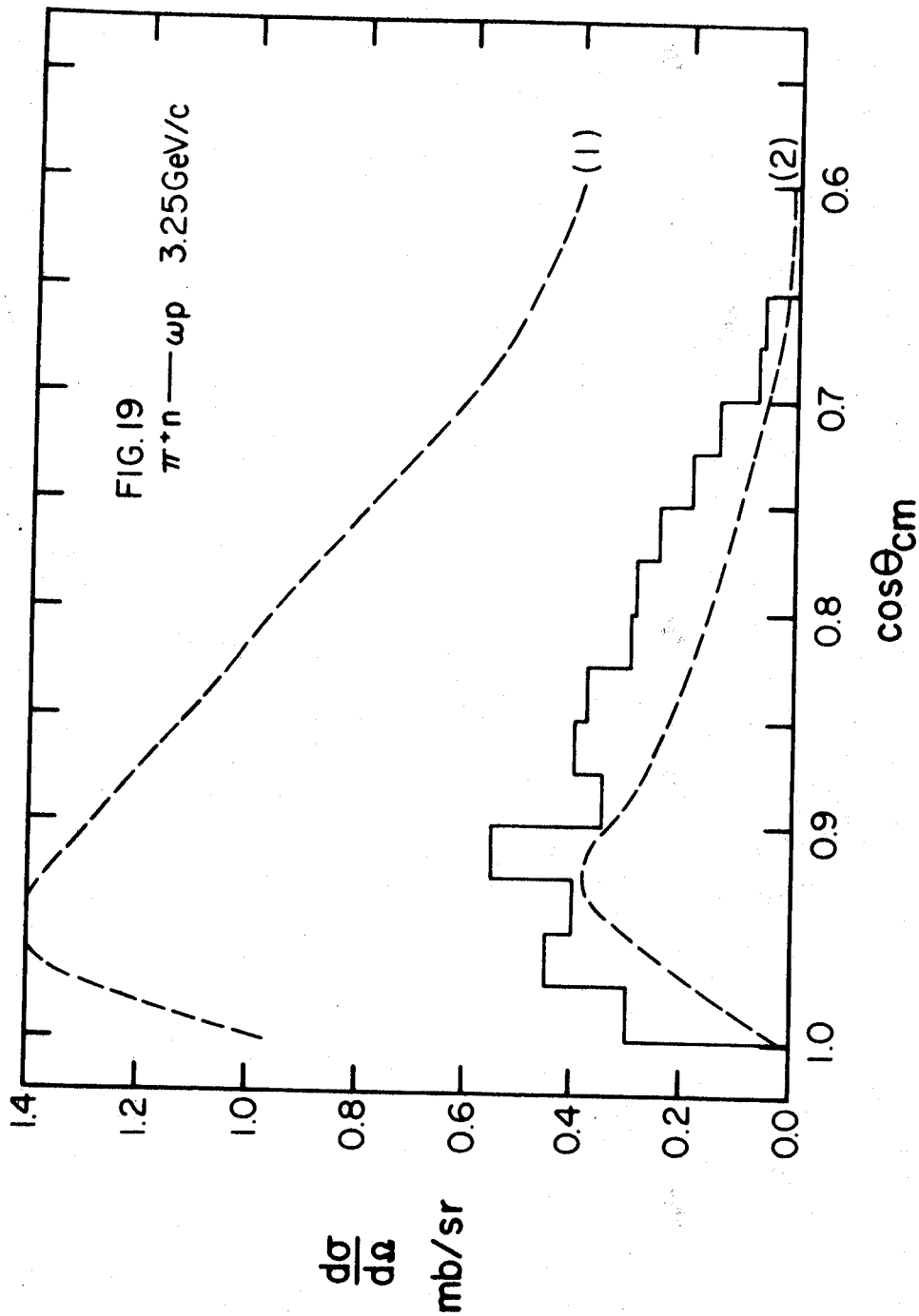

Figure 19. Comparison of theory and experiment for the vertex correction graph for $\pi n \rightarrow \omega p$.

Here we can have interference and reference to the calculational details for the separate terms shows that the corrections to the BTM helicity amplitudes are such that we could obtain a prediction for the denity matrix elements. However, absorptive BTM gives us this already and there is still the problem of energy dependence. There are, of course, still the other fourth order contributions of this type, diagrams 17c, for example, as well as others. These other graphs are plagued by severe divergence problems and the non-divergent terms show no improvement in the energy dependence. The conclusion is that vertex corrections are not the answer to the energy dependence problem, so one must try other things.

There is currently much interest in the relationship between absorptive corrections and Regge poles; most of it devoted to justifying simultaneous use of the two models. The idea is to write a Regge form for the inelastic interactions and apply absorptive corrections.

We will see that such calculations can be successful. There is, however, one other alternative to be considered.

Two-Pion Exchange

We abandon the BTM and guess, perhaps, that only pions can be exchanged in the interaction. The ω resonance is assumed to be produced by sequential pickup of two virtual pions. The simplest relevant Feynman graphs are shown in Figure 20. Note that this time we have 6 contributing graphs.

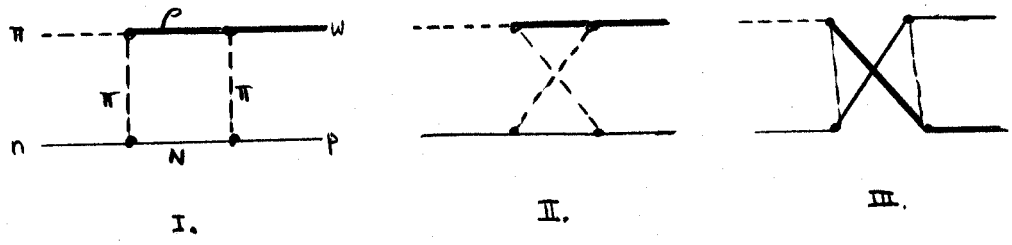

Figure 20. Simple two pion exchange diagrams for the reaction $\pi n \to \omega\rho$.

As before, using the usual rules, one obtains expressions for the matrix elements:

$$\langle\lambda\mu'|M^{I}|\mu\rangle_n = 2\sqrt{2}\, G^2 \frac{f}{M_c}\varepsilon_{\lambda\nu\rho\sigma}a_\lambda q\ \varepsilon^*_\sigma(c,\lambda)\bar{u}(d,\mu')\gamma_5\Lambda^{\pm}_\rho\gamma_5 u(b,\mu) \quad q=b-d$$

$$\langle\lambda\mu'|M^{II}|\mu\rangle_n = \text{----------}\Lambda^{II}_\rho$$

$$\langle\lambda\mu'|M^{III}|\mu\rangle_n = \text{----------}a_\lambda r_\nu\varepsilon^*_\sigma(d,\lambda)\bar{u}(c,\mu')\gamma_5\Lambda^{III}_\rho\gamma_5 u(b,\mu) \quad r=b-c$$

with

$$\Lambda^{I}_\rho = \Delta_{n\rho}\int\frac{d^4e}{(2\pi)^4}\ \frac{e_\rho}{[e^2+M_\pi^2]\,[(a+e)^2+M_e^2]\,[(q-e)^2+M_\pi^2]\,[(b-e)^2+M^2]}$$

+ other terms and obtain II by the replacement $a\to -c$ in Λ^I and III by the replacement $q\to r$ in Λ^I.

It is necessary to be very careful when making approximations to be sure the dominant contributions are retained. We assume, however, that the contribution from III can be neglected relative to I and II.

Reference to Appendix IV shows that we can write (using the same notation as for the vertex correction calculation)

$$\gamma_5\Lambda^{I}_\rho\gamma_5 = \Delta_{np}L^{(4)}_{\mu\nu}(M_p) + i\gamma_\lambda[L^{(4)}_{\mu\nu}(M_n) - L^{(4)}_{\mu\nu}(M_p)]$$

$$L^{(n)}_{\rho\mu\text{--}}(M) = \int ds' \int\frac{d^4p}{(2\pi)^4}\ \frac{p_\rho p_\mu p_{\text{---}}}{[e^2-2ep_z+p_z^2]^n}$$

A seemingly endless number of algebraic manipulations leads to a compact form for the scattering amplitudes. We obtain

$$\langle\lambda\mu'|T^{I}|\mu\rangle_n = iKB^{\lambda}\{\mu',\mu\}I[yz] - iKB\frac{W_{\mu'\mu}}{\Delta_{np}}I_3 - KM^{\lambda}_{\mu'\mu}J/\Delta np \quad I=I_1-I_2$$

Similar expressions can be written for the T^{II} and T^{III} terms. Here K contains coupling constants, and miscellaneous factors of and has the same definition as in the vertex correction amplitude.

The other factors are

$$B^{\lambda}=\frac{i}{\sqrt{2}}qq'\sin\theta_{cm}\delta_{\lambda,\pm 1} \qquad W_{\mu'\mu}=i\bar{U}(d,\mu')\not{A}U(b,\mu)$$

$$\{\mu'_{\lambda}\mu\} = \bar{U}(d,\mu')U(b,\mu) \qquad M^{\lambda}_{\mu'\mu}=\bar{U}(d,\mu')\not{N}^{\lambda}U(b,\mu)$$

$$N=\epsilon_{\lambda\nu\rho\sigma}a_{\lambda}q_{\nu}\varepsilon^{*}_{\sigma}(c,\lambda)$$

Rewriting in terms of the fourth order parameter functions $F_i(x,z)$ for convenience in investigating the energy dependence, we have.

$$I_1=\frac{\pi^2}{(2\pi)^4}\int dzdxz^2(1-z)F_i(x,z)_{Mp}$$

$$I_2=\frac{\pi^2}{(2\pi)^4}\int dzdxz^3(1-z)\{[F_1(x,z)+\frac{M_p}{\Delta_{np}}F_2(x,z)]_n - [F_1(x,z)+\frac{M_p}{\Delta_{np}}F_2(x,z)]_{Mp}\}$$

$$I_3=\frac{\pi^2}{(2\pi)^4}\int dzdxz^2(1-z)^2(1-x)[F_1(x,z)M_n-F_1(x,z)_{Mp}]$$

$$J+\frac{\pi^2}{(2\pi)^4}\int dzdx(1-z)z[F_4(x,z)M_n-F_4(x,z)M_p]$$

The energy dependence of the F's is discussed in the Appendix, as is that of the other factors. We find that F_1, $F_2 \sim S^{-2}$ and $F_4 \sim S^{-1}$ so I, I_2, $I_3 \sim S^{-2}$ and $J \sim S^{-1}$.

Similarly, examination of the expressions for $W_{\mu',\mu}$ and $M^{\lambda}_{\mu',\mu}$ gives S^1 and $S^{3/2}$, respectively, for the energy dependence. ($M_{\mu',\mu} \sim S^0$). Therefore we can write

$$T^I = a_1 + a_2\sqrt{s}$$

Squaring, etc. leads to an expression for $\frac{dr}{d\Omega}$

$\frac{dr^I}{d\Omega} = a + \frac{b}{\sqrt{s}} + \frac{c}{s}$ const. (one can obtain similar results for I and III).

This result is obviously much more pleasing that the BTM and its simple vertex corrections; there is at least some reason to be optimistic about 2π-exchange. The t-behavior can be seen easily in Figure 21, which shows $ReI_1^{(I)}$ and $ImI_1^{(I)}$ as a function of CM scattering angle for incident pion momenta of 3.25GeV/c. Note the predominant forward peak and absence of any backward peak. It should be noted that the peak in the cross section will be shifted away from the forward direction because of the influence of angular factors in the kinematics. Figure 22 shows the same information with the $T^{(II)}$ contribution added, eg. $Re(I_1-\bar{I}_1)$ and $Im(I_1-\bar{I}_1)$. The $T^{(II)}$ contribution is about 1/30 of $T^{(I)}$ in magnitude. It is clear that $T^{(II)}$ could have been neglected.

The term proportional to J (J looks like I but is of opposite sign) provides a small correction which additively effects the helicity amplitudes and can therefore give a non-BTM density matrix prediction, but at these energies this correction is not noticable. Figure 23

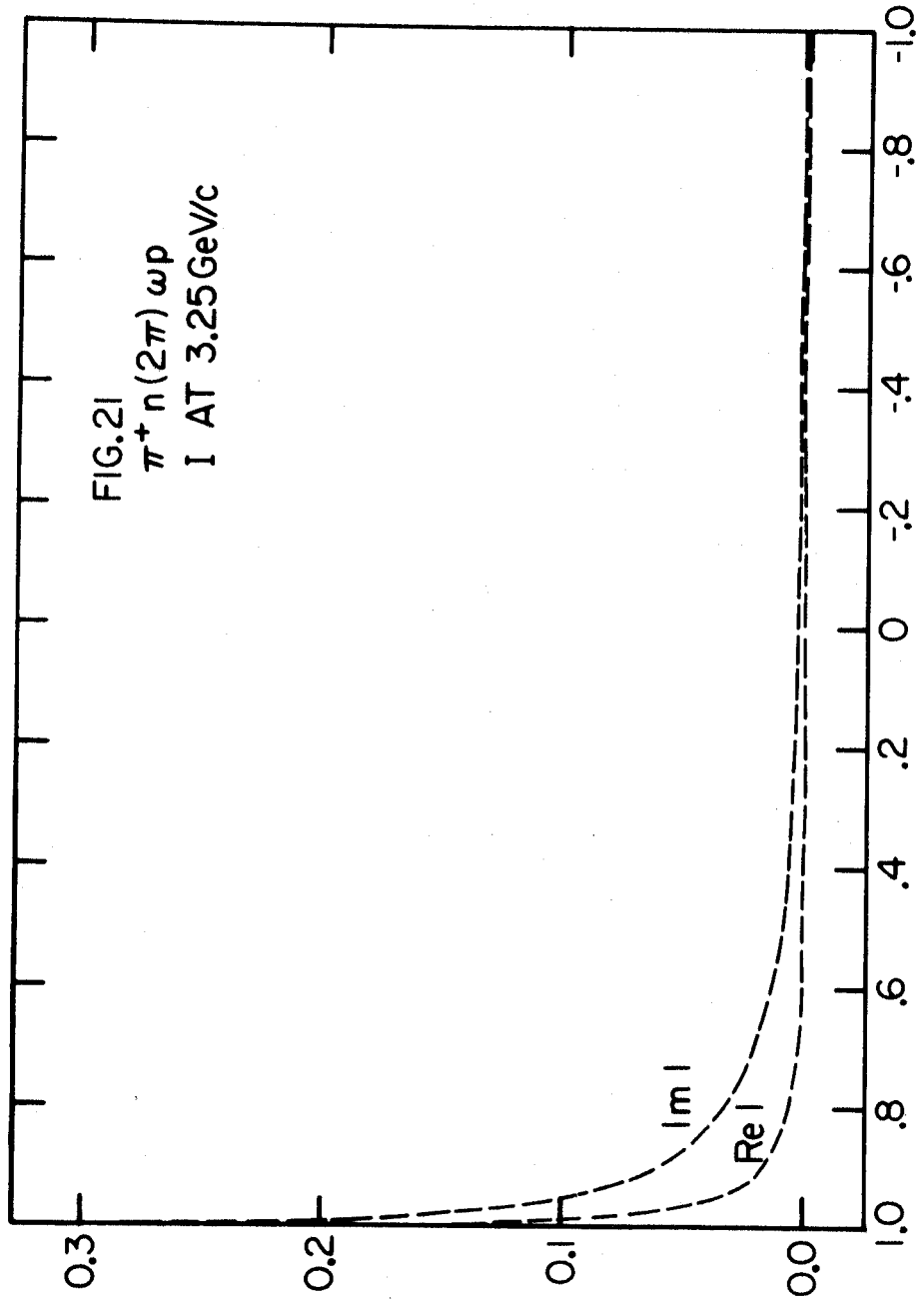

Figure 21. Re $I_1^{(I)}$ and Im $I_1^{(I)}$ over the physical range of t for the reaction $\pi n \to \omega p$ at 3.25 GeV/c.

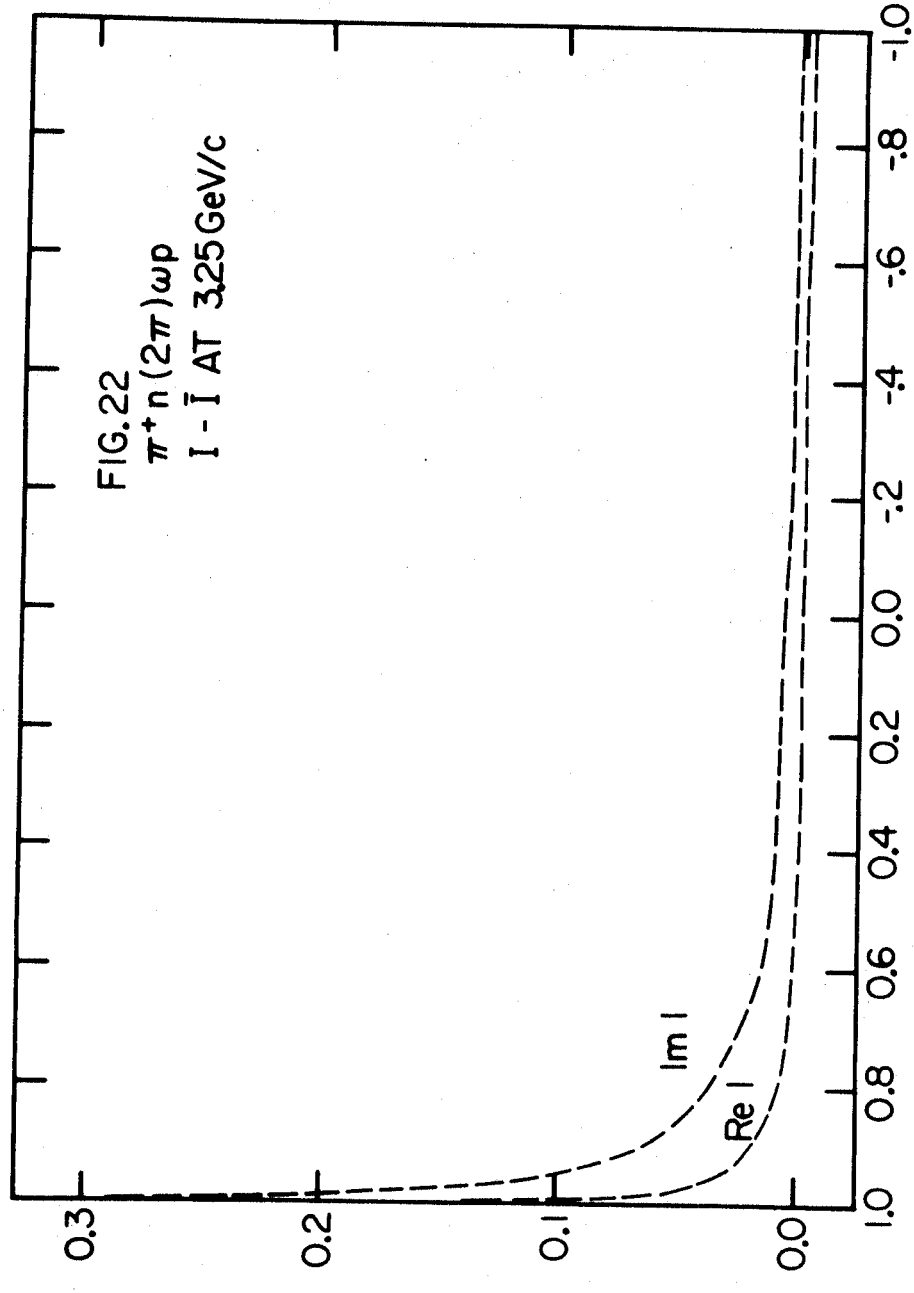

Figure 22. $Re(I_1-\bar{I}_1)$ and $Im(I_1-\bar{I}_1)$ over the physical range of t for the reaction $\pi n \to \omega p$ at 3.25 GeV/c.

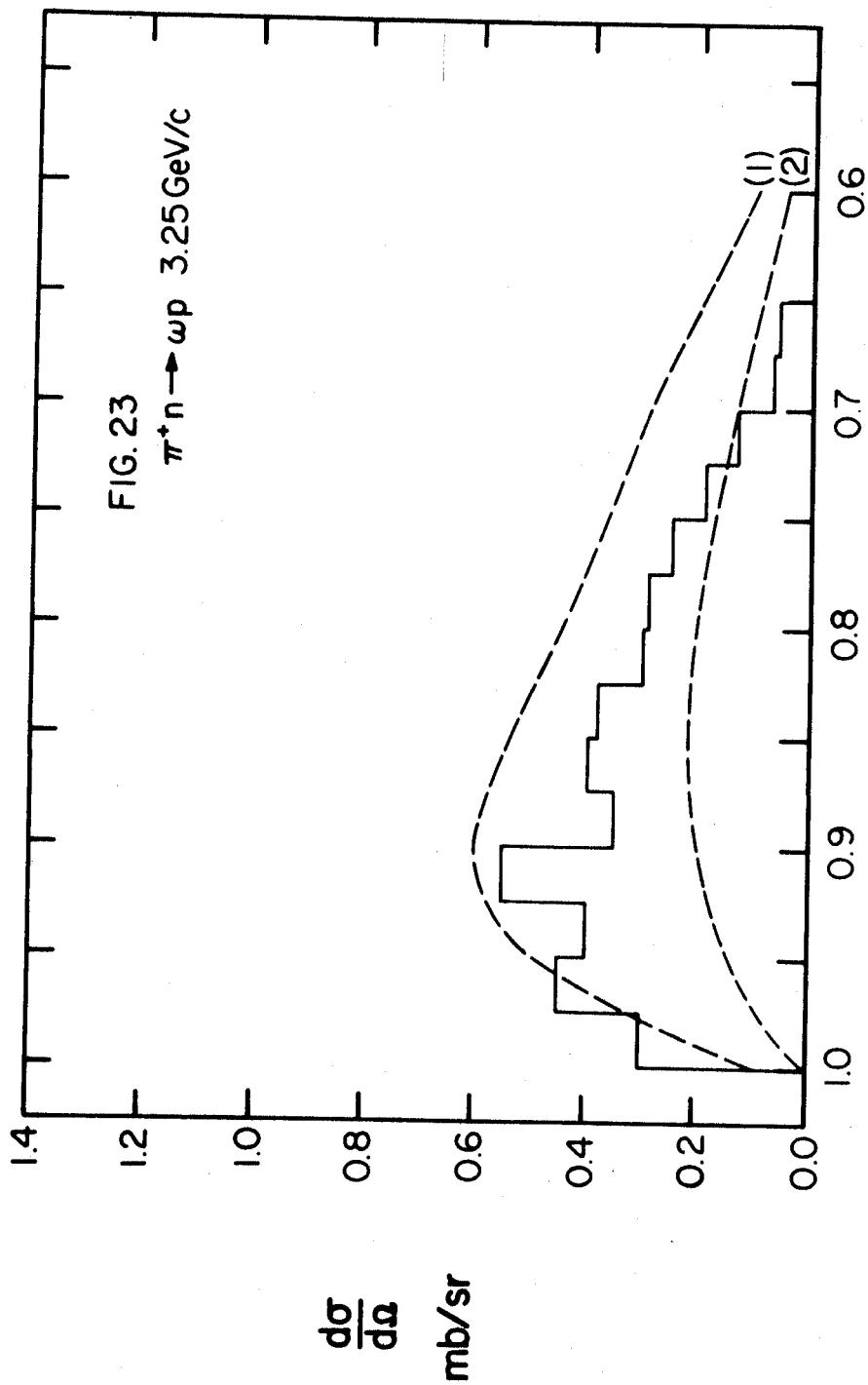

Figure 23. $\frac{d\sigma}{dt}$ vs. t for the reaction $\pi n \rightarrow \omega p$ assuming 2π-exchange as the dominant mechanism.

shows the angular distribution assuming 2π exchange for the production mechanism. Absorptive corrections have been included, the result is acceptable. The conclusion is that 2π exchange can work and give an acceptable energy dependence. Cursory examination of final states containing higher spin resonant states shows that 2π exchange will break down, ie. predict an incorrect energy dependence, but that $n\pi$ exchange for some appropriate n will restore the prediction to an acceptable value. It is interesting that sums of exchange graphs can give Regge energy behavior. Also absorption is clearly a different physical effect from multiparticle exchange. The argument that the physical effects behind Regge exchange and absorption are distinct has recently been given in detail by Marc Ross, Frank Henyey, and Gordon Kane.[11]

ABSORPTIVE REGGE MODEL

We accept the qualitative arguments against double counting and apply absorptive corrections to the Regge exchange amplitudes for the reaction np→pn assuming dominance of the π,ρ,A_2 trajectories. This reaction is interesting because of the availability of experimental data for the cross section and an experiment now in progress to measure the final neutron asymmetry, ie. a polarization. If the cross section for this reaction (and related reactions) can be fit in a consistent manner then one obtains a prediction for the polarizations.

Regge poles have definite spin and parity[12] and the Regge model tells us that the trajectories with the largest $\alpha(t)$ will dominate the amplitude at high energy. The conservation laws tell us that the exchange quanta must be members of non-strange isotopic spin triplets of mesons; π,ρ,A_2 are acceptable candidates. We must determine how these trajectories contribute to various t-channel helicity amplitudes.

Expanding in t-channel partial waves we have

$$\langle\lambda_2\lambda_4|T(t,\theta_t)|\lambda_1\lambda_3\rangle_{n_t}=\Sigma_j(2j+1)\langle\lambda_2\lambda_4|T^j(t)|\lambda_1\lambda_3\rangle_{n_t} d^j_{\lambda_t\mu_t}(\theta_t)$$

$$\lambda_t=\lambda_1-\lambda_3$$

$$\mu_t=\lambda_2-\lambda_4$$

$$n_t=\lambda_t-\mu_t$$

In np charge exchange $\lambda_1=\lambda_2=\lambda_3=\lambda_4=1/2$, giving a total of 16 helicity amplitudes. Application of parity conservation and time reversal invariance reduces this number to 6. Further, strong interactions are I-spin invariant so we neglect the n-p mass difference and kinematically we have identical particle scattering which gives one more relation and so reduces the number of independent helicity amplitudes to these five:

$$\phi_d^t=\langle 1/2\ 1/2|T|1/2\ 1/2\rangle_0$$

$$\phi_2^t=\langle 1/2\ 1/2|T|-1/2\text{-}1/2\rangle_0$$

$$\phi_3^t=\langle 1/2\text{-}1/2|T|1/2\text{-}1/2\rangle_0$$

$$\phi_4^t=\langle 1/2\text{-}1/2|T|-1/2\ 1/2\rangle_2$$

$$\phi_5^t=\langle 1/2\ 1/2|T|1/2\text{-}1/2\rangle_1$$

To determine the Regge contribution to each amplitude we write the amplitudes as linear combinations of parity conserving amplitudes (Regge poles have definite parity), expand these into partial waves (definite spin assoc. with each trajectory) and perform the Sommerfield-Watson transform to obtain the appropriate Regge forms. After removing kinematic singularities we obtain (after long and tedious algebra)

$$\phi_1^t = 1/2 \sum_i (\beta_{00}^{i+} + \beta_{00}^{i-}) \zeta_i (s/s_0)^{\alpha^i}$$

$$\phi_2^t = 1/2 \sum_i (\beta_{00}^{i+} - \beta_{00}^{i-}) S_i (s/so)^{\alpha i}$$

$$\phi_3^t = 1/2 \sum_i \alpha_i (\beta_{11}^{i+} + \beta_{11}^{i-}) S_i (s/so)^{\alpha i}$$

$$\phi_4^t = -1/2 \sum_i \alpha_i (\beta_{11}^{i+} - \beta_{11}^{i-}) S_i (s/so)^{\alpha i}$$

$$\phi_5^t = 1/2 \sin\theta_t \sum_i \beta_{10}^{i+} S_i (s/so)^{\alpha_i - 1}$$

where ζ_i is the usual signature factor, $\alpha_i(t)$ is the i^{th} Regge trajectory, and the $\beta_{\lambda\mu}^{i\pm}$ are the residue functions, (the $\pm$ refer to $\binom{\text{natural}}{\text{unnatural}}$ parity).

We see immediately that the ρ and A_2, both natural parity particles, can contribute to all of the amplitudes. The π, unnatural parity, contributes only to β_{00}^{i-} and therefore only to ϕ_1^t and ϕ_2^t such that $\phi_1^{t\pi pole} = -\phi_2^{t\pi pole}$. With faith that our ϕ_i^t contain only dynamical singularities we apply crossing to obtain the s-channel amplitudes:[13]

$$\langle \lambda_c \lambda_d | T | \lambda_a \lambda_b \rangle^s = \sum d^{1/2}_{\lambda', a\lambda_a}(\chi_t)\, d^{1/2}_{\lambda', b\lambda_b}(\pi - \chi_t)\, d^{1/2}_{\lambda', c\lambda_c}(\pi - \chi_t)$$

$$d^{1/2}_{\lambda', d\lambda_d}(\chi_t) \langle \lambda'_c \lambda'_a | T | \lambda'_d \lambda'_b \rangle^t$$

where $$\cos\chi_t = [s/(s-4M^2)]^{1/2} [t/(t-4M^2)]^{1/2}$$

After much calculating we obtain

$$\phi_1^s = 1/2\sin^2\chi_t [\phi_1^t + \phi_2^t + \phi_3^t + a\phi_4^t + 4b\phi_5^t] \qquad a = \frac{1+\cos^2\chi}{\sin^2\chi}$$

$$\phi_2^s = 1/2\sin^2\chi_t [\phi_1^t - a\phi_2^t + \phi_3^t - \phi_4^t + 4b\phi_s^t] \qquad b = \cot\chi$$

$$\phi_3^s = 1/2\sin^2\chi_t [\phi_1^t + \phi_2^t - a\phi_3^t - \phi_4^t + 4b\phi_s^t]$$

$$\phi_4^s = 1/2\sin^2\chi_t [a\phi_1^t - \phi_2^t - \phi_3^t + \phi_4^t - 4b\phi_5^t]$$

$$\phi_5^s = 1/2\sin^2\chi_t [-b(\phi_1^t + \phi_2^t + \phi_3^t - \phi_4^t) + 2(1-b^2)\phi_s^t]$$

Reference to the expressions for ϕ_i^t shows that only ϕ_2^s and ϕ_4^s contains the π pole. One readily obtains

$$\phi_2^{s\pi\text{pole}} = \phi_4^{s\pi\text{pole}} = 1/2\bar{\beta}^\pi S_\pi (s/s_0)^{\alpha_\pi}$$

Now, ϕ_4^π is an n=2 amplitude, ie. net helicity transfer from the incident to the final state is 2 units of angular momentum, and must therefore vanish like (-t) as $t \to 0$. Therefore we conclude that

$$\bar{\beta}^\pi = (-t)\beta^\pi$$

and the π pole cannot possible contribute to the experimentally observed forward peak. In Figure 24a we see the $^\pi$pole amplitude as a function of t.

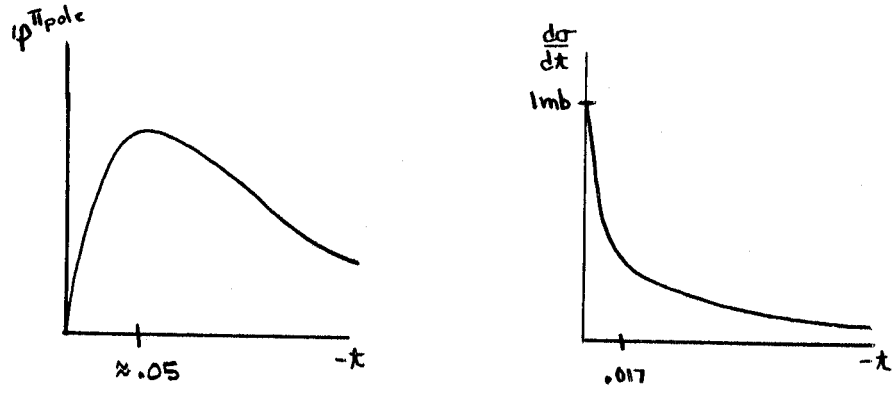

Figure 24. Sketches of (a) π pole amplitude and (b) experimental t angular distribution for np pn at 8 GeV/c.

Since the π pole is nearest to the physical region it is expected to be the dominant contribution to the cross section. The conclusion is that the Regge pole model predicts a dip in the forward direction in np charge exchange. (Figure 24b shows the shape of the experimental $d\sigma/dt$.)

There is a way around this difficulty.[14] Until now the solution has been to assume the existence of a <u>parity doublet</u> for the π. We require a second π trajectory, π^d, of positive parity which <u>conspires</u> with the π such that $\phi_4^{\pi+\pi^d}=0$, as required by conservation of angular momentum, without the necessity for $\phi_2^{\pi+\pi^d}=0$.

The π^d contributes to ϕ_2^s and ϕ_4^s with opposite sign so we obtain

$$\phi_2^{s\pi+\pi^d}=1/2\bar{\beta}^{\pi}s_{\pi}(s/so)^{\alpha^{\pi}}+1/2\bar{\beta}^{\pi^d}s_{\pi d}(s/so)^{\alpha\pi^d}$$

$$\phi_4^{s\pi+\pi^d}=1/2\bar{\beta}^{\pi}s_{\pi}(s/so)^{\alpha^{\pi}}-1/2\bar{\beta}^{\pi^d}s_{\pi d}(s/so)^{\alpha\pi^d} \qquad s_{\pi}=s_{\pi}d$$

Now angular momentum conservation gives

$$\phi_4^{s\pi+\pi^d}(t=0)=0 \qquad \text{(the } \rho \text{ and } A_2 \text{ contributions vanish at } t=0\text{)}$$

$$\rightarrow \quad \bar{\beta}^{\pi}(t=0)=\bar{\beta}^{\pi d}(t=0)$$

$$\alpha_n(t=0)=\alpha_{\pi d}(t=0)$$

and we see that $\phi_2^{s\pi+\pi^d}$ need not vanish at t=0 and the existence of the π pole at $t=M_\pi^2\simeq 0$ insures a large contribution in the forward direction.

It is true that the ρ, A_2 contributions to ϕ_1^s, and ϕ_3^s do not have to vanish in the forward direction as indicated in Figure 25. However, the amplitudes are rather smooth and flat, slowly decreasing, functions of t. When the π pole is added and the other amplitudes

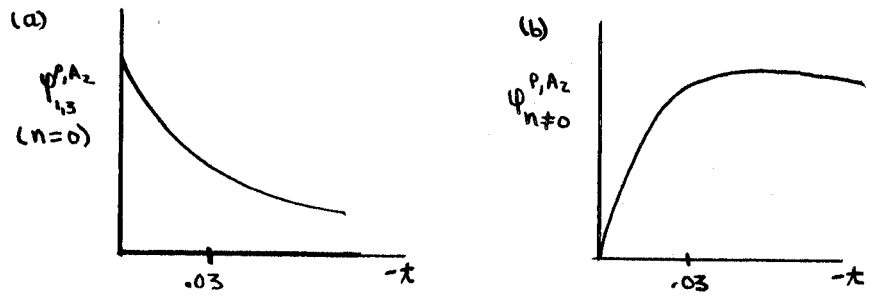

Figure 25. Sketches of ρ and A_2 contributions to (a) n=0 and (b) $n\neq 0$ amplitudes in the reaction $\pi p\rightarrow pn$.

are considered the combined effect is to produce a dip in the forward cross section; the presence of the π^d trajectory remedies this defect.

One problem with the conspiracy solution is that the π^d is not observed so its introduction becomes a non-physical extension of the model. We will see that application of absorptive corrections introduces cuts associated with each pole, each containing positive and negative parity parts, and that the behavior of the π cut in the forward direction is effectively that of the conspirator so we explain the data in a physical way.

We look at the absorptive formula derived earlier:

$$\langle\lambda_c\lambda_d|T^A|\lambda_a\lambda_b\rangle_n=\langle\lambda_c\lambda_d|T^B|\lambda_a\lambda_b\rangle_n$$

$$+iN\sum_j(2j+1)d^j_{\lambda\mu}(\theta)\{\langle\lambda_c\lambda_d|T^{EL}_j|\lambda_1\lambda_2\rangle\langle\lambda_1\lambda_2|T^B_j|\lambda_a\lambda_b\rangle$$

$$+\langle\lambda_c\lambda_d|T^B_j|\lambda_1\lambda_2\rangle\langle\lambda_1\lambda_2|T^{EL}_j|\lambda_a\lambda_b\rangle\} \text{ -----}$$

where, as is usual, the absorptive interactionsin the incident and final channels are assumed equal. Using of the Jacob-Wick expansion and the elastic scattering parameterization

$\langle\lambda_c\lambda_d|T^{EL}|\lambda_a\lambda_b\rangle=-4q^2(i+\rho)\sigma_T\rho^{At/2}\delta_{\lambda_c\lambda_a}\delta_{\lambda_d\lambda_b}$ where

σ_T=total cross section and $\rho=\mathrm{Re}T^{EL}/I_mT^{EL}$ are

experimentally determined as is **A.**

one obtains

$$\langle\lambda_a\lambda_b|T^A|\lambda_a\lambda_b\rangle_n=\langle\lambda_c\lambda_d|\pi^B|\lambda_a\lambda_b\rangle_n+K_1\rho^{At/2}\int_{-\infty}^{0}dt'\rho^{At'/2}I_n(A\sqrt{tt'})$$

$\langle\lambda_c\lambda_d|T^B|\lambda_a\lambda_b\rangle_n$ with $K_1=-\frac{\sigma T}{4\pi A}(1-i\rho)$.

The Born pole term or Regge pole term T^B enters in the second term which is a superposition of several poles, ie. a cut. Thus to each pole there is associated a cut generated by the absorptive correction to the amplitude. The cut is not a parity eigenstate and so contains both natural and unnatural parity parts. This means that we can have interesting polarization effects, "self-conspiracy" etc. The important point is that the cut term could, and so we shall see does, have the same effect as the introduction of conspiring trajectories. eg., np charge exchange: the $\phi_2{}^{cut}$ need <u>not</u> vanish at t=0.

We fix the π-residue by equating, in the high energy limit, the Born term to the Regge contribution at the π pole. With π pole + π-cut most of the very forward cross section is reproduced. Figure 26 shows $\frac{d\sigma}{dt}$ vs t at 8 GeV/c with the experimental data.[15] The same procedure of equating Regge form and Born term at the pole for the ρ meson is used. First we look at πN charge exchange and use factorization of residues to determine the ratio of non-flip to flip ρ residues. Extrapolation to the Born term of np charge exchange then fixes the magnitudes and signs of the residues in a consistent manner in terms of the vector and tensor coupling constants of vector mesons to baryons. (np charge exchange Born term is enough by itself but πN charge exchange allows separation of residues into vertex parts and provides a consistency check).

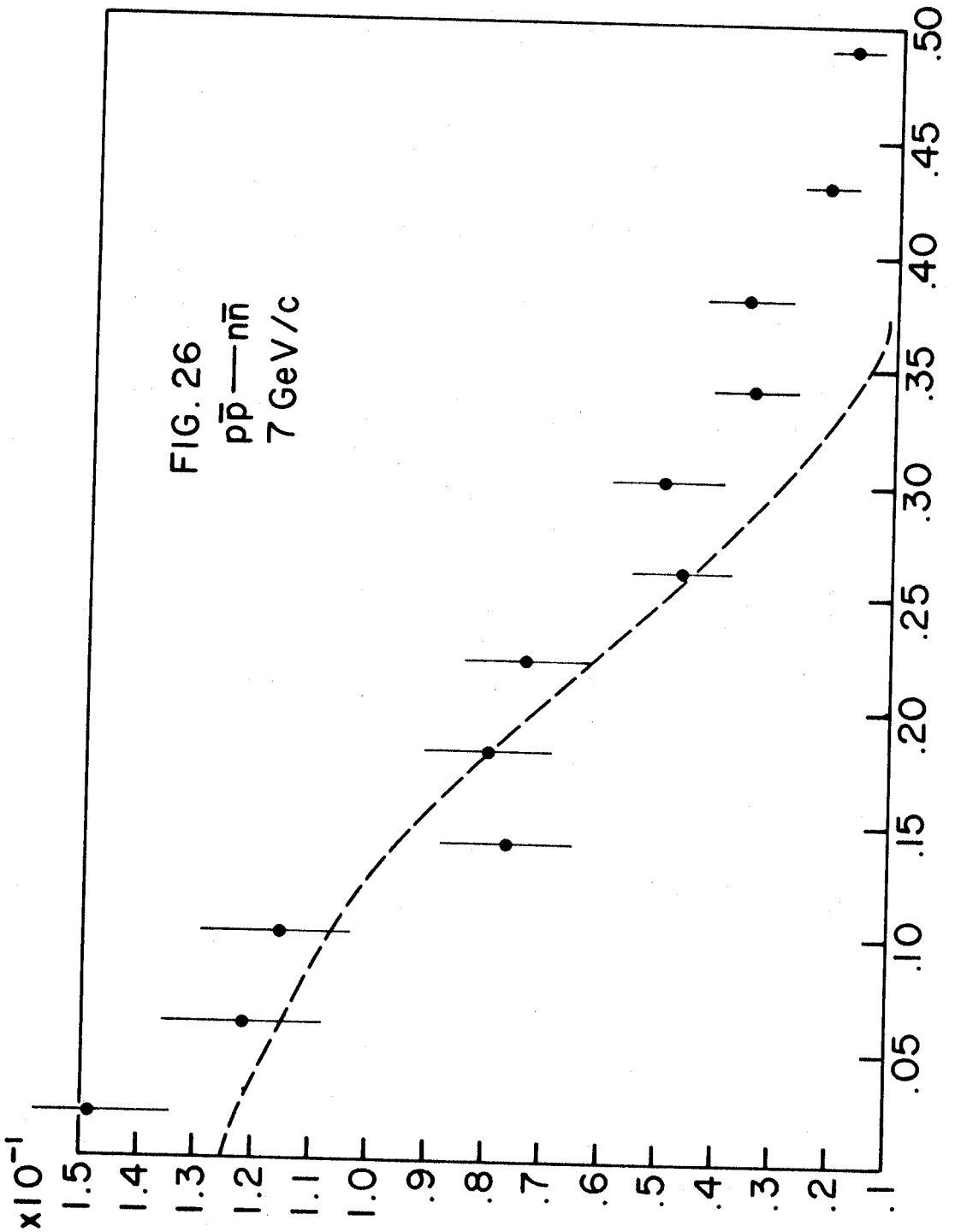

Figure 26. $\frac{d\sigma}{dt}$ vs. t for $np \rightarrow pn$ at 8 GeV/c. (Data are from G. Manning et al A.E.R.E. Harwell, England)

We set the relative sign of the ρ and A_2 by requiring the $(\rho+A_2)$ contribution to an amplitude by predominantly real. (The ρ and A_2 are treated as exchange degenerate. Experimentally $\frac{d\sigma}{dt}(np\to pn)$ holds its shape to low energies, ie. no resonance formation). Since the signs of the π and ρ are fixed by the Born terms, all signs are determined absolutely.

The procedure was to fix π pole + π cut to reproduce the break in $\frac{d\sigma}{dt}$ and add ρ and A_2 to get a best fit to the overall t-distribution by varying the values of G_V and G_T for the ρ and A_2 within physically acceptable limits. The procedure uniquely fixes the polarizations.

The experiment now in progress measures the recoil neutron asymmetry by using a polarized proton target. A simple calculation determines this polarization in terms of the ϕ_t^s to be

$$A=2NIm\phi^{s-*}_5(\phi_1^s+\phi_2^s+\phi_3^s-\phi_4^s) \quad N^{-1}=[|\phi_1^s|^2+|\phi_2^s|^2+|\phi_4^s|^2+|\phi_5^s|^2]\alpha\ \frac{d\sigma}{dt}$$

A close look at the contributions of the various poles and cuts to the expression shows

1. $\phi_5^s\simeq\sqrt{-t}\phi_5^s$
2. $\phi_1^s+\phi_2^s+\phi_3^s-\phi_4^s$ does not contain the π pole

We expect the π cut to dominate at small t because of the proximity of the π pole to the physical region, and therefore attribute the sharp forward peak to this contribution. We suspect that $\frac{d\sigma}{dt}\ A/\sqrt{t}$ will be relatively flat. Calculations clearly support these conjectures. Figure 27 shows the results of the calculations.

There is one last point to be examined. Analysis of the reaction, $p\bar{p}\to n\bar{n}$ shows that it has the same t-channel as np charge exchange, and therefore must be dominated by the same poles. Application of the G-parity operator to the two reactions shows that we obtain the $p\bar{p}\to n\bar{n}$ amplitudes by changing the sign of the ρ contribution to the charge exchange. Consistency requires a good fit to $p\bar{p}\to n\bar{n}$ with the same parameters. Figure 28 compares the theoretical fit to the experimental data for $p\bar{p}\to n\bar{n}$ at 7 GeV/c.[16] The fit is quite good so we conclude that this model is a good one.

While other approaches to this problem of np charge exchange can be successful, we believe that absorptive corrections to Regge pole amplitudes has strong appeal from a physical point of view. It is certainly a more satisfying explanation than introduction of spurious trajectories and arbitrary vanishing of residues to satisfy experiment. We have faith that attempts to fit other high energy inelastic reactions with this model will prove successful. Only time will tell.

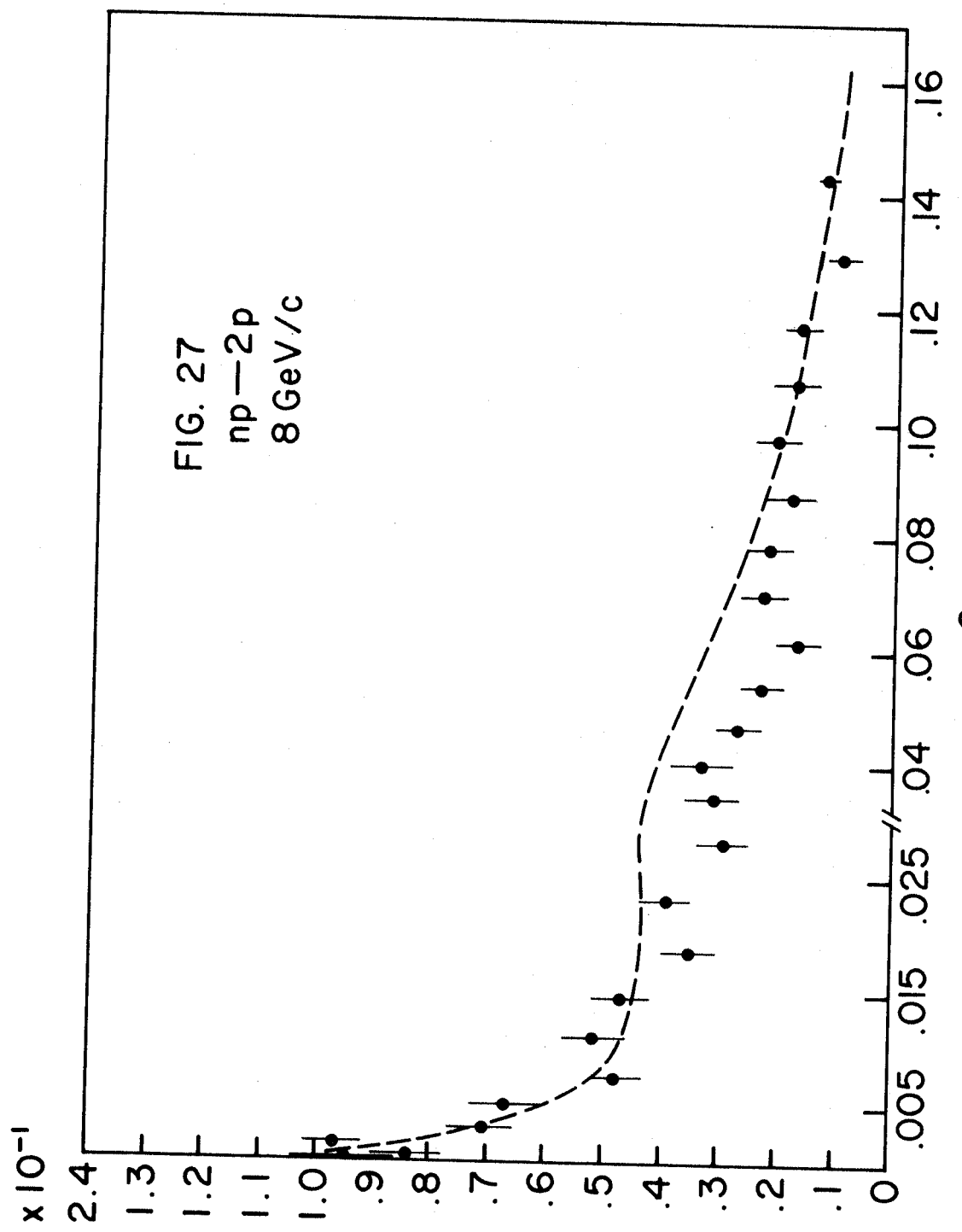

Figure 27. $\frac{d\sigma}{dt}$ vs. t for $p\bar{p} \to n\bar{n}$ at 7 GeV/c. (Data are from P. Astbury et al. Phys. Lett. 16 (1965) 328).

REFERENCES

1. M. Jacob and G. C. Wick, Annals of Phys. 7,(1959)404.

2. R. J. Glauber, Lect. in Theo. Phys. Vol. 1, Boulder 1958, Interscience Publishers.

3. J. D. Jackson, J. T. Donohue, K. Gottfried, R. Keyser, B. E. Y. Svensson, Phys. Rev. 139(1965)B428.

4. J. D. Jackson, Rev. Mod. Phys. 37(1965)484.

5. J. D. Jackson and H. Pilkuhn, Nuovo Cimento, Series X, 33(1964)906.

6. A. Amaldi and F. Selleri, Nuovo Cimento 31,(1964)360.

7. S. C. Frautschi, M. Gell-Mann, F. Zachariasen, Phys. Rev. 126(1962)2204.

8. B. Margolis and A. Rotsstein, Preprint McGill Univ. 1968.

9. D. Griffiths, R. J. Jabbur, Preprint Wayne State Univ. 1968.

10. S. Frautschi, B. Margolis, CERN Preprint Th.909, 1968.

11. F. Henyey, G. L. Kane, Jon Pumplin, M. H. Ross, Univ. of Mich. Preprint, 1969.

12. M. Gell-Mann, M. L. Goldberger, F. E. Low, E. Marx, F. Zachariasen, Phys. Rev. 133(1964)B145.

References (continued)

13. T. L. Trueman and G. C. Wick, Annals of Physics 26(1964)322.

14. L. Bertocchi, Heidelberg International Conference on Elementary Particles, North-Holland Publishers, 1968.

15. J. V. Allaby, F. Binon, A. N. Diddens, et al., Submitted to XIII Int. High Energy Conf., Vienna 1968.

16. E. W. Anderson, E. J. Bleser, et. al., Submitted to Phys. Rev. Letts.

APPENDIX

APPENDIX I

Notation and Kinematics

1. For the diagram shown in Figure 28, a,b,c,d,e are the 4-momenta of the particles of mass M_a, M_b, M_c, M_d, M_e, respectively. The metric is such that scalar products are written $ab = -a_0b_0+\underline{a}\cdot\underline{b} = a_4b_4+\underline{a}\cdot\underline{b}$.

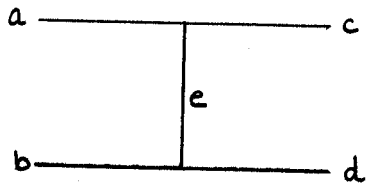

Figure 28. Feynman diagram of OPE contribution to ab→cd scattering.

2. Whenever convenient we use the Mandelstam variables s,t,u given by

$$S = -(a+b)^2 = -(c+d)^2$$
$$t = -(b-d)^2 = -e^2 = -(c-a)^2$$
$$u = -(a-d)^2 = -(c-b)^2.$$

These variables are not independent; energy-momentum conservation leads to $s+t+u = M_a^2+M_b^2+M_c^2+M_d^2$

3. Figure 29 shows the orientations of the 4-momenta relative to the coordinate axes in the s-channel center-of-mass system

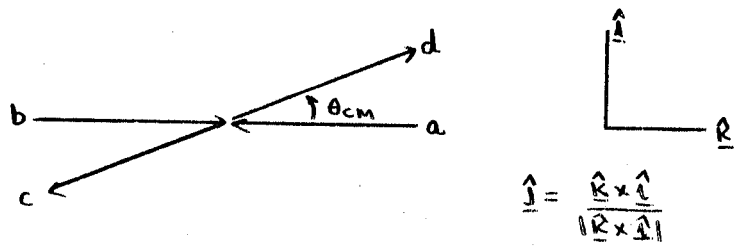

Figure 29. The s-channel center-of-mass system for ab→cd scattering

With this orientation, the 4-vectors for the momenta take the form

$$a_u = (a_0, o, o, -q) \qquad c_u = (c_0, -q'\sin\theta, o, -q'\cos\theta)$$
$$b_u = (b_0, o, o, q) \qquad d_u = (d_0, q'\sin\theta, o, q'\cos\theta)$$

4. It is convenient to define the complete symmetric function $\lambda(x,y,z)$:

$$\lambda(x,y,z) = x^2+y^2+z^2-2xy-2xz-2yz.$$

Using this function we obtain

$q = \frac{1}{2\sqrt{s}}\,\lambda^{1/2}(s, M_a^2, M_b^2)$ = incident channel CM momentum

$q' = \frac{1}{2\sqrt{s}}\,\lambda^{1/2}(s, M_c^2, M_d^2)$ = final channel CM momentum

$a_c = \frac{1}{2M_c}\,\lambda^{1/2}(t, M_a^2, M_c^2)$ = magnitude of 3-momentum of a in c rest frame

$b_d = \frac{1}{2M_d}\,\lambda^{1/2}(t, M_b^2, M_d^2)$ = magnitude of 3-momentum of b in d rest frame

Other useful kinematic quantities are easily cast into this compact form.

5. We write the Dirac equation for spin-1/2 particles as $(i\gamma\cdot x+M)U=0$ and normalize the spinors as $\bar{U}U=2M$. The γ-matrices are defined such that $\gamma^{+}=\gamma$ and $\gamma_5=\gamma_1\gamma_2\gamma_3\gamma_4=i\gamma_1\gamma_2\gamma_3\gamma_0$. The quantity $\sigma_u=-i[\gamma_u,\gamma]$ is also used frequently. Using these γ's and referring to the CM coordinates we obtain the following positive energy spinors: $(U(x,\lambda_x)$=pos. E. spinor of 4-momentum x and helicity $\lambda_x)$ $N(x)=(x_0-M_x)^{1/2}$

$$U(b,1/2) = N(b)\begin{bmatrix} 1 \\ 0 \\ \frac{q}{b_0+M_b} \\ 0 \end{bmatrix} = N(b)\begin{bmatrix} 1 \\ \frac{q}{b_0+M_b} \end{bmatrix}\begin{bmatrix} 1 \\ 0 \end{bmatrix} = N(b)\begin{bmatrix} 1 \\ \frac{q}{b_0+M_b} \end{bmatrix}\chi_{1/2}$$

$$U(b,-1/2) = N(b)\begin{bmatrix} 1 \\ \frac{-q}{b_0+M_b} \end{bmatrix}\begin{bmatrix} 0 \\ 1 \end{bmatrix} = N(b)\begin{bmatrix} 1 \\ \frac{-q}{b_0+M_b} \end{bmatrix}\chi_{-1/2}$$

$$U(d,1/2) = N(d)\begin{bmatrix} 1 \\ \frac{-q}{d_0+M_d} \end{bmatrix}(\chi_{1/2}\cos\theta/2 + \chi_{-1/2}\sin\theta/2)$$

$$U(d,-1/2) = N(d)\begin{bmatrix} 1 \\ \frac{-q'}{d_0+M_d} \end{bmatrix}(\chi_{-1/2}\cos\theta/2 - \chi_{1/2}\sin\theta/2)$$

$$U(a_1 1/2) = N(a)\begin{bmatrix} 1 \\ \frac{q}{a_0+M_a} \end{bmatrix}\chi_{-1/2}$$

$$U(a,-1/2) = N(a)\begin{bmatrix} 1 \\ -\frac{q}{a_0+M_a} \end{bmatrix} \chi_{1/2}$$

$$U(c,1/2) = N(c)\begin{bmatrix} 1 \\ -\frac{q'}{c_0+M_c} \end{bmatrix} (\chi_{-1/2}\cos\theta/2 - \chi_{1/2}\sin\theta/2)$$

$$U(c_1,-1/2) = N(c)\begin{bmatrix} 1 \\ -\frac{q'}{c_0+M_c} \end{bmatrix} (\chi_{1/2}\cos\theta/2 + \chi_{-1/2}\sin\theta/2)$$

We use these spinors to calculate useful scalar products:

(a) $(\lambda_d,\lambda_b) = \bar{U}(d,\lambda_d)\gamma_5 U(b,\lambda_b)$

$(1/2,1/2) = -(-1/2,-1/2) = -\zeta_-\cos\theta/2$

$(1/2,-1/2) = (-1/2,1/2) = \zeta_+\sin\theta/2 = \zeta_+\omega/2$

(b) $\{\lambda_d,\lambda_b\} = \bar{U}(d,\lambda_d)U(b,\lambda_b)$

$\{1/2,1/2\} = \{-1/2,-1/2\} = \psi_-\cos\theta/2$

$\{1/2,-1/2\} = -\{-1/2,1/2\} = \psi_+\sin\theta/2 = \psi_+\upsilon/2$

where

$$\zeta_\pm = [(b_0+M_b)(d_0+M_d)]^{1/2}\left(\frac{q}{b_0+M_b} \mp \frac{q'}{d_0+M_d}\right)$$

$$\psi_\pm = [(b_0+M_b)(d_0+M_d)]^{1/2}\left(1+\frac{q}{b_0+M_b}\frac{q'}{d_0+M_d}\right)$$

Similar quantities $\zeta'_\pm, \psi'$ can be defined for scalar products involving spin 1/2 particles a,c

(c) The following products are also useful:

1) $W_{\lambda_d\lambda_b} = i\bar{U}(d,\lambda_d)\not{a}U(b,\lambda_b)$ $\qquad W_{++}=W_{--}=(a_0\psi_+-q\zeta_+)$

$\qquad\qquad\qquad\qquad\qquad\qquad\qquad\qquad W_{+-}=-W_{-+}=(-a_0\psi_-+q\zeta_-)\omega/2$

2) $M^{\lambda_c}_{\lambda_d\lambda_b}=\bar{U}(d,\lambda_d)\not{N}^{\lambda_c}U(b,\lambda_b)$ with $N^{\lambda_c}_{\mu}=\varepsilon_{\lambda\nu\mu\sigma}a_\lambda e\ \varepsilon^*_\sigma(c,\lambda_c)$

The 4-vector ε_μ is a spin 1 polarization vector. It is discussed in Section 6.

$$M^1_{++}=M^{-1}_{--}=-\frac{1}{\sqrt{2}}\zeta_+(qc_0+q'a_0)\omega^3-\frac{1}{\sqrt{2}}\zeta_+a_0q'\omega+\frac{1}{\sqrt{2}}\psi_+qq'\omega$$

$$M^0_{++}=-M^0_{--}=-\frac{1}{2}\zeta_+qM_c\omega^2$$

$$M^{-1}_{++}=M^1_{--}=-\frac{1}{\sqrt{2}}\zeta_+qc_0\omega+\frac{1}{\sqrt{2}}\psi_+qq'\omega$$

$$M^1_{+-}=-M^{-1}_{-+}=\sqrt{2}\zeta_-(qc_0-q'a_0)-\frac{1}{2\sqrt{2}}\zeta_-a_0q'\omega^2+\frac{1}{2\sqrt{2}}\psi_-qq'\omega^2=-M^{-1}_{-+}$$

$$M^0_{+-}=M^0_{-+}=-qM_c\zeta_-\omega$$

$$M^{-1}_{+-}=-M^1_{-+}=\frac{1}{2\sqrt{2}}\zeta_-qc_0\omega^2+\frac{1}{2\sqrt{2}}\psi_-qq'\omega^2$$

All of these expressions are small angle approximations; only the lowest powers of ω are retained.

6. Specification of spin-1 states is in terms of polarization 4-vectors $\varepsilon_\mu(c,\lambda_c)$ subject to the subsidiary condition $c\cdot\varepsilon=0$ and defined such that

$$\varepsilon_\mu(c,\lambda)\varepsilon_\mu(c,\lambda')=\delta_{\lambda\lambda'},\quad \varepsilon_\mu(c,\lambda)\varepsilon_\nu(c,\lambda)=\delta_{\mu\nu}+\frac{c_\lambda c_\nu}{M_c^2}$$

Refering to the CM coordinates, if

(a) particle c is spin 1

$$\varepsilon(c,+1)=\frac{1}{\sqrt{2}}[o,\cos\theta,-i,-\sin\theta]$$

$$\varepsilon(c,o)=\frac{1}{M_c}[q',-c_0\sin\theta,o,-\cos\theta]$$

$$\varepsilon(c,-1)=\frac{1}{\sqrt{2}}[o,\cos\theta,-i,-\sin\theta]$$

(b) particle d is spin 1

$$\varepsilon(d,+1)=\frac{1}{\sqrt{2}}[o,-\cos\theta,-i,\sin\theta]$$

$$\varepsilon(d,o)=\frac{1}{M_d}[q',d_0\sin\theta,o,d_0\cos\theta]$$

$$\varepsilon(d,-1)=\frac{1}{\sqrt{2}}[o,\cos\theta,-i,-\sin\theta]$$

7. For particles of spin greater than 1, we use the Rarita-Schwinger formalism and construct high spin wave functions by the angular momentum addition theorem subject to subsidiary conditions:

Example: spin 3/2

$$U_\mu(d,\lambda_d)=\langle 1\lambda\, 1/2\bar{\lambda}\,|\,3/2\lambda_d\rangle\varepsilon_\mu(d,\lambda)U(d,\bar{\lambda})$$

$$\gamma_\mu U_\mu=0 \qquad d_\mu U_\mu=0$$

Expanding, we obtain

$$U_\mu(d,3/2)=\varepsilon_\mu(d,+1)U(d_1 1/2)$$

$$U_\mu(d,1/2)=\frac{1}{\sqrt{3}}\varepsilon_\mu(d,+1)U(d,-1/2)+\sqrt{\frac{2}{3}}\varepsilon_\mu(d,o)U(d,1/2)$$

The other two spinors can be obtained by changing the signs of the helicities.

8. We rewrite the propagator $\frac{1}{M_e^2-t}$ to make the dependence on $\omega=2\sin\theta/2$ more transparent:

$$M_e^2-t=M_e^2+(b-d)^2=-(b_0-d_0)^2+(q-q')^2+qq'\omega^2+M_e^2$$

now

$$s=(a+b)^2=(a_0+b_0)^2$$

so write

$$(b_0-d_0)^2=\frac{1}{4s}\,[2(b_0-d_0)(a_0+b_0)]^2$$

$$=\frac{1}{4s}[(b_0-d_0)(a_0+b_0+c_0+d_0)]^2 \qquad \text{using } a_0+b_0=c_0+d_0$$

$$=\frac{1}{4s}[(b-d)(b+d)+(c-a)(c+a)]^2$$

$$=\frac{1}{4s}[(M_d^2-M_b^2)+(M_c^2-M_a^2)]^2$$

which leads to

$$M_e^2-t=M_e^2+(q-q')^2-\frac{1}{4s}[(M_d^2-M_b^2)+(M_c^2-M_a^2)]^2+qq'\omega^2=qq'\varepsilon^2+qq'\omega^2$$

which defines ε^2

and gives us $[M_e^2-t]^{-1}=\frac{1}{qq'}\,\frac{1}{\varepsilon^2+\omega^2}$ which we use frequently in absorption calculations of OPE diagrams.

One can procede in the same way for u-channel exchanges to obtain

$$\frac{1}{M_e^2-U}=\frac{1}{qq'}\,\frac{1}{\varepsilon_u^2+\omega_u^2}$$

with

$$qq'\varepsilon_u^2=M_e^2+(q-q')^2-\frac{1}{4s}[(M_d^2-M_a^2)+(M_b^2-M_c^2)]^2$$

9. For cross section calculations we use

$$S=1-i(2\pi)^4\delta(p_f-p_i)\left[\pi_i(2E_i)\right]^{-1}M \text{ as our S-matrix}$$

and obtain

$$\frac{d\sigma}{d\Omega}=\frac{1}{64\pi^2 s}\frac{q'}{q}\frac{1}{(2S_a+1)(2S_b+1)}\sum_{\text{spin}}|\langle\lambda_c\lambda_d|M|\lambda_a\lambda_b\rangle|^2$$

and

$$\frac{d\sigma}{dt}=\frac{\pi}{qq'}\frac{d\sigma}{d\Omega}\,.$$

APPENDIX II

Calculation Details: OME and Modifications for $\pi^+ n \to \omega p$

In the center-of-mass we arrange the coordinate system as shown in Figure 30.

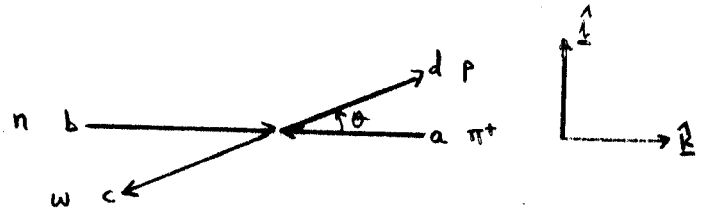

Figure 30. Coordinate system for OME calculation of $\pi^+ n \to \omega p$.

Using this geometry we easily write the energy-momentum 4-vectors of the particles.

$$a=(a_0,0,0,-q)$$

$$b=(b_0,,),q)$$

$$c=(c_0,-q'\sin\theta,0,-q'\cos\theta)$$

$$d=(d_0,q'\sin\theta,0,q'\cos\theta)$$

Application of the Feynmann rules leads to an expression for the helicity amplitudes M:

$$\langle\lambda_c\lambda_d|M|\lambda_b\rangle_n \qquad n=|(\lambda_c-\lambda_d)+\lambda_b|$$

$$=\frac{f_{\pi\rho\omega}}{M_\omega} G_V Z\bar{U}(d,\lambda_d)A_\mu N_\mu^{\lambda_c} U(b,\lambda_b)$$

where $Z=[M_\rho^2-t]^{-1}$, $f_{\pi\rho\omega}$ is the PVV coupling constant and G_V is the vector BVB coupling constant.

$$A_\mu=i\gamma_0[\eta\gamma_\mu+2i\Lambda\eta d_\mu] \qquad \Lambda=(M_b+M_d)^{-1}$$

$$N_\mu=\varepsilon_{\mu\nu\rho\sigma}a_\nu\rho_\rho\varepsilon_\sigma^*\ (c,\lambda_c) \qquad \eta'=1+\frac{G_T}{G_V}=1+\eta$$

G_T=tensor BVB coupling

$\varepsilon(c,\lambda_c)$ is the ω-meson polarization 4-vector

Expanding and using the center-of-mass vectors a,b,c,d, we obtain

$$A_\mu N_\mu=-A_0a_3c_1\varepsilon_2^*+A_1(a_3c_0-a_0c_3)\varepsilon_2^*+A_2[(a_0c_3-a_3c_0)\varepsilon_1^*-a_0c_1\varepsilon_3^*$$
$$+a_3c_1\varepsilon_0^*]+A_3a_0c_1\varepsilon_2^*$$

So one can write

$$\langle\lambda\mu'|M|\mu\rangle\sim\ [-A_0^{\mu'\mu}E^\lambda+A_1^{\mu'\mu}F^\lambda+A_2^{\mu'\mu}G^\lambda+A_3^{\mu'\mu}H^\lambda]$$

where $A_\eta^{\mu'\mu}=\bar{U}(d,\mu')A_\eta U(b,\mu)$

It is necessary to calculate only half of the amplitudes because $\langle-\lambda-\mu'|M|-\mu\rangle=-(-)^n\langle\lambda\mu'|M|\mu\rangle$ which comes from invariance principles. (Inversion of the y-axis in connection with parity conservation gives this relation)

The factors A are easily evaluated:

$$A_0^{++}=A_0^{--}=i[-\eta'\psi_++2\Lambda\eta\psi_-d_0]\cos\theta/2$$

$$A_0^{+-}=-A_0^{-+}=i[-\eta'\psi_-+2\Lambda\eta\psi_+d_0]\sin\frac{\theta}{2}$$

$$A_1^{++}=A_1^{--}=i[4\Lambda\eta q'\psi_-\cos^2\frac{\theta}{2}-\eta'\zeta_+]\sin\frac{\theta}{2}$$

$$A_1^{+-}=-A_1^{-+}=i[4\Lambda\eta q'\psi_+\sin^2\frac{\theta}{2}+\eta'\zeta_-]\cos\frac{\theta}{2}$$

$$A_2^{++}=-A_2^{--}=\eta'\zeta_+\sin\frac{\theta}{2}$$

$$A_2^{+-}=A_2^{-+}=\eta'\zeta_-\cos\frac{\theta}{2}$$

$$A_3^{++}=A_3^{--}=i[2\Lambda\eta q'\psi_-\cos\theta-\eta'\zeta_+]\cos\frac{\theta}{2}$$

$$A_3^{+-}=-A_3^{-+}=i[2\Lambda\eta q'\psi_+\cos\theta-\eta'\zeta_-]\sin\frac{\theta}{2}$$

also: $E=\frac{i}{\sqrt{2}}qq'\sin\theta=-\frac{q}{a_0}H^{\pm}$ $\quad E^0=F^0=H^0=0$ $\quad G^0=-qM_e\sin\theta$

$$F=\frac{i}{\sqrt{2}}[qc_0-q'a_0\cos\theta] \quad G^{\pm}=\pm\frac{1}{\sqrt{2}}[qc_0\cos\theta-a_0q']$$

It is convenient to rewrite all of the angular factors in terms of $\omega=2\sin\frac{\theta}{2}$. Then we form the amplitudes as

$$\langle\lambda\mu'|M|\mu\rangle_n=\theta ZA_\mu N_\mu=\theta Z\sum_{\ell=n} x_{a\ell}\omega^{\ell+2}=B_n^a$$

where the index a numbers amplitudes of a given helicity transfer n and

$$\theta=\frac{f}{M_\omega}G_v$$

It is now a simple matter to obtain the scattering amplitudes in a particular model.

1. The Born Term Model (BTM)

   Calculate the cross section using the amplitudes as they stand.

2. Born Term with Form Factor (BTMF)

   Let $Z=(M_\rho^2-t)^{-1}F(s,t)$ and calculate using the BTM expression for the amplitudes.

3. Reggeized Propagator Model (BTMR)

Follow the procedure discussed in the Regge Model section; let

$$Z=\frac{2\pi\alpha'(t0)}{(2j+1)[\tau+(-)^j]}(2\alpha(t)+1)\frac{1-e^{-i\pi\alpha(t)}}{2\sin\pi\alpha(t)}$$

$$\left\{\frac{S-1/2(M_a^2+M_b^2+M_c^2+M_d^2)}{2M_a(M_bM_d)^{1/2}}\right\}^{\alpha(t)-1}$$

and use the BTM expression.

4. The Absorptive Model (BTMA)

Let DW(x) be the absorptive function. Then, neglecting terms in ω higher than ω^{n+2},

$$B_n^a=\frac{\theta}{qq'}[(X_{an}-\varepsilon^2\bar{X}_{an})\varepsilon^n\int_{J_0}^{x_u}xdxJ_n(\omega x)k_n(\varepsilon x)DW(x)$$

$$+\omega^n\bar{X}_{an}DW(J_0)]$$

where we have used the identity $\frac{\omega^n}{\varepsilon^2+\omega^2}$

$$=\varepsilon^n\int_{J_0}^{\infty}xdx\ J_n(\omega x)K_n(\varepsilon x).$$

In an actual calculation the upper limit will have to finite--one simply chooses xu large enough to get most of the amplitude. J_0 is the lowest allowed partial wave: $J_0=\text{Max}[|\lambda_c-\lambda_d|,|\lambda_a-\lambda_b|]$. The error in this change is small. This short cut as mentioned already is only good for modifications to the plain BTM.

APPENDIX III

BVB Vertex Corrections

We consider only the two simplest graphs as shown in Figure 31.

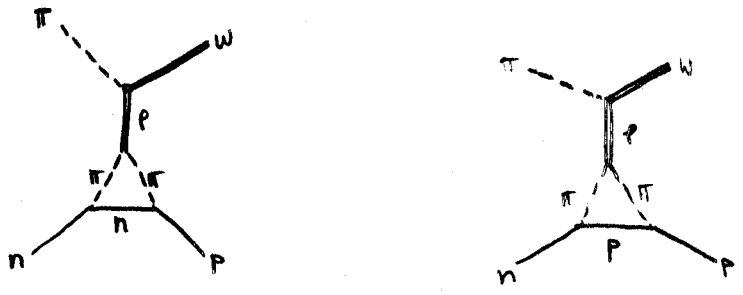

Figure 31. Diagrams giving vertex corrections to NρN point vertex.

Using the Feynman Rules we obtain an expression for the helicity amplitudes:

$$\langle \lambda_c \lambda_d | M | \lambda_b \rangle = \sqrt{2} G^2_{NNP} g_{PPV} \frac{f_{VVP}}{M_c} \frac{1}{M_\rho^2 - t} \varepsilon_{\mu\nu\rho\sigma} a_\nu e_\rho \varepsilon^*_\sigma(c, \lambda_c)$$

$$\bar{U}(d, \lambda_d) \gamma_5 \Lambda_\mu \gamma_5 U(b, \lambda_b)$$

where

$$\Lambda_\mu = \int \frac{d^4 \ell}{(2\pi)^4} \frac{2\ell_\mu}{(\ell^2 + M_\pi^2)((e-\ell)^2 + M_\pi^2)} \left\{ \frac{1}{i(\not{b} - \not{\ell}) + M_p} - \frac{1}{i(\not{b} - \not{\ell}) + M_n} \right\}$$

the following parameterization facilitates simplification of the integrand;

$$\frac{1}{\ell^3+M_\pi^2}\,\frac{1}{\ell^2-2e\ell+\Delta_2}\,\frac{1}{\ell^2-2b\ell+\Delta_3} = \frac{1}{\ell^2+M_\pi^2}\int_0^1 dy \frac{1}{[\ell^2-2ep_y+\Delta_y]^2}$$

$$= \int_0^1 2(1-Z)\,dz\,dy \frac{1}{[\ell^2-2ep_Z+\Delta_Z]^3}$$

ds

$\Delta_2=e^2+M_\pi^2=M_\pi^2-t$ $\qquad P_y=e+dy$

$\Delta_y=\Delta_2(1-y)+\Delta_3 y$ $\qquad \Delta_3=b^2+M^2$

$P_Z=P_y(1-Z)$ $\qquad =by(1-Z)+e(1-y)(1-Z)$

$\Delta_2=\Delta_y(1-Z)+M_\pi^2$

Rearranging and using $(i\not{p}+M)u(P)=0$

we obtain

$$\Lambda_\mu=-2\Delta npL^{(3)}(M_p)+2i\gamma_\lambda[L^{(3)}_{\lambda\mu}(M_n)-L^{(3)}_{\lambda\mu}(M_p)] \qquad \Delta_{np}=M_b-M_d$$

$$=M_n-M_p$$

with

$$L^{(3)}_{\lambda\mu}(M)=\int ds\int\frac{d^4\ell}{(2\pi)^4}\,\frac{\ell_\mu\ell_\nu}{[\ell^2-2eP_Z+\Delta_Z]^3}$$

$L^{(3)}_{\mu\nu}$ contains one finite and one divergent term.

Write $\ell=\ell'+P_Z$ and obtain

$$L_{\mu\nu}(M)=\int ds\int\frac{d^4\ell'}{(2\pi)^4}\,\frac{\ell'_\mu\ell'_\nu+\ell'_\mu P_Z+\ell'_\nu P_{Z\mu}+P_{Z\mu}P_{Z\nu}}{[\ell'^2+\Delta_Z-P_Z^2]^3}$$

The term odd in ℓ' vanishes and the quadratic term is divergent (or, more correct, the integral does not exist). Allowing a liberal interpretation of the rules for manipulating infinities we write for the 2nd term in Λ_μ

$$2i\int ds \not{p}_z P_z \int \frac{d^4\ell'}{(2\pi)^4}\left\{\frac{1}{[\ell'^2+\Delta_z(M_p)-P_z^2]^3} - \frac{1}{[\ell'^2+\Delta_z(M_n)-P_z^2]^3}\right\}$$

recall

$$P_z = by\,z + e(1-y)\,z \qquad \text{(have let } z \to 1-z\text{)}$$

so we can write

$$\bar{U}(d)\,i\not{P}_z U(b) = -M_b\,yz\bar{U}(d)U(b) - (M_b - M_d)(1-Y)\,z\bar{U}(d)U(b)$$

$$= -M_d\,yz \qquad -\Delta_{np}\,z\bar{U}(d)U(b)$$

Using this expression we obtain

$$\Lambda_\mu = -2ib_\mu\Delta_{np}\{K_1[yz] + 2\frac{M_d}{\Delta_{np}}K_1'[y^2z^2] + 2K_1''[yz^2]\} = -2ib_\mu\Delta_{np}K[yz]$$

with

$$K_1[yz] = \frac{\pi^2}{(2\pi)^4}\int dz F_3(1,z)_{M_p}$$

$$K_1'[y^2z^2] = \frac{\pi^2}{(2\pi)^4}\int dz\; z[F_5(1,z)_{M_n} - F_5(1,z)_{M_p}]$$

$$K_1''[yz^2] = \frac{\pi^2}{(2\pi)^4}\int dz\; z[F_3(1,z)_{M_n} - F_3(1,z)_{M_p}]$$

(the y integrations have been performed analytically. Please refer to the discussion of the parameter functions F_i).

Substituting, we obtain

$$<\lambda_c\lambda_d|T|\lambda_b>_n = i\theta Z B^{\lambda}\{\lambda_d,\lambda_b\}K[yz] \qquad \theta = 2\sqrt{2}G^2 g\frac{f}{M_c}\Delta_{np}$$

$$Z = [M_\rho^2 - t]^{-1}$$

$$B^{\lambda}\ b\cdot N = \varepsilon_{\mu\nu\rho\sigma} b_\mu a_\nu c_\rho \varepsilon^*_\sigma(c,\lambda_c)$$

$$= -qq'\sqrt{s}\,\varepsilon^*_2(c,\lambda) \text{ in CM system}$$

which gives

$$<0\ 1/2|T|\ 1/2>_0 = 0$$

$$<1\ 1/2|T|-1/2>_0 = \frac{1}{2\sqrt{2}}\theta\psi_+\sqrt{\frac{\omega^2}{\varepsilon^2+\omega^2}}\,K[yz]$$

$$<0-1/2|T|1/2>_1 = 0$$

$$<1\ 1/2|T|\ 1/2>_1 = \frac{1}{\sqrt{2}}\theta\psi_-\sqrt{\frac{\omega}{\varepsilon^2+\omega^2}}K[yz]$$

$$<1-1/2|T|-1/2>_1 = <1\ 1/2|T|\ 1/2>_1$$

$$<1-1/2|T|\ 1/2>_2 = -<1\ 1/2|T|-1/2>_0$$

These amplitudes can be used to calculate cross sections in the usual way.

APPENDIX IV

Two Meson Exchange in PB→VB

The relevant diagrams (the simplest) are shown in Figure 32.

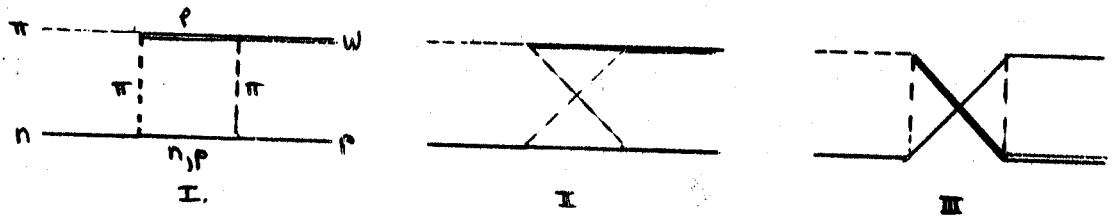

Figure 32. Two pion exchange graphs for $\pi^+ n \to \omega\rho$.

Using the Feynman rules and proceding in the usual manner we obtain

$$T^{I}=2\sqrt{2}\; G^2_{NN\pi} g_{\pi\pi\rho} \frac{f_{\pi\rho\omega}}{M_c} \varepsilon_{\lambda\nu\rho\sigma}\; a_\lambda q_\nu \varepsilon^*_\sigma(c)\bar{U}(d)\gamma_5 \Lambda^I_\mu \gamma_5 U(b) \qquad q=b-d$$

$$T^{II}=-2\sqrt{2}\; G^2_{NN\pi} g_{\pi\pi\rho} \frac{f_{\pi\rho\omega}}{M_c} \varepsilon_{\lambda\nu\rho\sigma}\; a_\lambda q_\nu \varepsilon^*_\sigma(c)\bar{U}(d)\gamma_5 \Lambda^{II}_\mu \gamma_5 U(b)$$

$$T^{III}=-2\sqrt{2}\; G^2_{NN\pi} g_{\pi\pi\rho} \frac{f_{\pi\rho\omega}}{M_d} \varepsilon_{\lambda\nu\rho\sigma}\; a_\lambda r_\nu \varepsilon^*_\sigma(d)\bar{U}(c)\gamma_5 \Lambda^{III}_\mu \gamma_5 U(b) \qquad r=b-c$$

with

$$\Lambda_\mu^I=\Delta_{np}\int\frac{d^4e}{(2\pi)^4}\frac{e_\mu}{[e^2+M_e^2][(a+e)^2+M_n^2][(q-e)^2+M_g^2][(b-e)^2+M_p^2]}$$

$$+i\gamma_\lambda\frac{d^4e}{(2\pi)^4}\frac{e_\mu e_\lambda}{[e^2+M_e^2][(a+e)^2+M_n^2][(q-e)^2+M_g^2]}\{\frac{1}{(b-e)^2+M_n^2}$$

$$-\frac{1}{(b-e)^2+M_p^2}\}$$

one obtains Λ_μ^I by the replacement $a\to -c$ in Λ_μ^I

and Λ_μ^{III} by the replacement $q\to r$ in Λ_μ^I

We rewrite Λ_μ and compress it by the use of parameter integrations $\frac{1}{ab}=\int_0^1 df\frac{1}{af+b(1-f)}$

to obtain

$$\gamma_5\Lambda_\mu\gamma_5=\Delta_{np}L^{(4)}(M_p)+i\gamma_\lambda[L_{\lambda\mu}^{(4)}(M_n)-L_{\lambda\mu}^{(4)}(M_p)]$$

where

$$L_{\mu\nu}^{(4)}=\int ds'\int\frac{d^4e}{(2\pi)^4}\frac{e_\mu e_\nu}{[e^2-2eP_z+P_z^2]^4}\qquad ds'=\frac{1}{(2\pi)^4}dxdydz\ z(1-z)$$

$$iP_z=iq\,z+idy\,z-ia(1-x)(1-z)$$

performing the loop integration we have (using the Dirac equation to simplify)

$$L_\mu^{(4)}(M_p)=id_\mu\int ds\frac{yz}{C^2(M_p)}$$

$$i\gamma_\mu L_{\lambda\mu}^{(4)}(M)=id_\mu\int ds\frac{yz}{C^2(M)}\not{P}_z+i\frac{1}{2}i\gamma_\lambda g_{\lambda\mu}\int ds\frac{1}{C(M)}\qquad ds=\pi^2 ds'$$

One can write

$$\bar{U}(d,\lambda_d)\,i\not{p}_z U(b,\lambda_b)=-\Delta_{np}Z\bar{U}U-M_\rho yz\bar{U}U-W_{\lambda_d\lambda_b}(1-x)(1-z)$$

$$W_{\lambda_d\lambda_b}=i\bar{U}(d)\not{\epsilon}U(b)$$

Putting all of the terms together we finally obtain

$$\bar{U}(d,\lambda_d)\gamma_5\Lambda^I_\mu\gamma_5 U(b,\lambda_b)=$$

$$id_\rho\Delta_{np}\Big[\int ds\frac{yz}{C^2(M_p)}-\int dsyz^2\Big(1+Y\frac{M_p}{\Delta_{np}}\Big)\Big(\frac{1}{C^2(M_n)}-\frac{1}{C^2(M_p)}\Big)$$

$$-\frac{W_{\lambda_d\lambda_b}}{\Delta_{np}}\int dsyz(1-x)(1-z)\Big(\frac{1}{C^2(M_n)}-\frac{1}{C^2(M\ )}\Big)\Big]$$

$$-\frac{1}{2}\bar{U}(d,\lambda_d)\gamma_\mu U(b,\lambda_b)\int ds\Big(\frac{1}{C(M_n)}-\frac{1}{C(M_p)}\Big)$$

which we rewrite as

$$id_\rho\Delta_{np}\Big\{I_1-I_2-\frac{W_{\lambda_d\lambda_b}}{\Delta_{np}}I_3\Big\}-\frac{1}{2}\bar{U}(d,\lambda_d)\gamma_\mu U(b,\lambda_b)J$$

where the definition of I_i and J is clear.

Substituting into the expression for T^I we finally obtain

$$\langle\lambda_c\lambda_d|T^I|\lambda_b\rangle=iKB^{\lambda c}\{\lambda_d,\lambda_b\}I-ikB^{\lambda c}\frac{W_{\lambda_d\lambda_b}}{\Delta_{np}}I_3-\frac{kM^{\lambda c}}{\Delta_{np}}{}_{\lambda_d\lambda_b}J$$

where $B^{\lambda c}=\frac{i}{\sqrt{2}}qq'\sqrt{s}\sin\theta_b d^\delta_{\lambda c,\pm 1}$ (in the CM)

$$\{\lambda_d,\lambda_b\}=\bar{U}(d,\lambda_d)U(b,\lambda_b) \qquad M^{\lambda c}_{\lambda_d\lambda_b}=\bar{U}(d,\lambda_d)\not{N}^{\lambda c}U(\lambda,\lambda_b)$$

$$W_{\lambda_d\lambda_b}=\bar{U}(d,\lambda_d)\ U(b,\lambda_b) \qquad N^{\lambda c}_\rho=\varepsilon_{\mu\nu\rho\sigma}a_\mu q_\nu\varepsilon^*_\sigma(c,\lambda_c)$$

$$K=2\sqrt{2}G^2g\frac{f}{M_c}\Delta_{np}$$

The integrel J is small than I_1, I_2, I_3 for moderate s but will eventually dominate as $s\to\infty$ since $J\sim s^{-1}$ and $I_i\sim s^{-2}$.

Performing the y-integration (parameter integral) analytically we get

$$I_1=\frac{\pi^2}{(2\pi)^4}\int dzdxz^2(1-z)F_1(x,z)M_p$$

$$I_2=\frac{\pi^2}{(2\pi)^4}\int dzdxz^3(1-z)\{[F_2(x,z)+\frac{M_p}{\Delta_{np}}F_2(x,z)]M_p\}$$

$$I_3=\frac{\pi^2}{(2\pi)^4}\int dzdxz^2(1-z)^2(1-x)[F_1(x,z)M_n-F_1(x,z)M_p]$$

$$J=\frac{\pi^2}{(2\pi)^4}\int dzdx(1-z)z[F_4(x,z)M_n-F_4(x,z)M_p]$$

Again, there are 12 amplitudes, 6 of them obtainable from the other six via symmetry considerations; the six independent amplitudes are

B_0^1 $\quad <01/2|T|1/2>_0 =-KM^0_{1/2\ 1/2}J/\Delta_{np} \qquad \sim s^0$

B_1^2 $\quad <11/2|T|1/2>_1 =-\frac{K}{\sqrt{2}}qq'\sqrt{s}\psi_-\omega[I-\frac{W_{1/2\ 1/2}}{\psi_-\Delta_{np}}I_3]$

$$-KM^1_{1/2\ 1/2}J/\Delta_{np} \qquad \sim s^{1/2}$$

$$=-\frac{K}{\sqrt{2}}qq'\sqrt{s}\psi_-\omega[I-\frac{(a_0\psi_+-q_+)}{\psi_-\Delta_{np}}I_3] \qquad \sim s^{1/2}$$

$$-KM^1_{1/2\ 1/2}J/\Delta_{np} \qquad \sim s^{1/2}$$

B_1^1 $\quad <0-1/2|T|1/2>_1=-KM^0_{-1/2\ 1/2}J/\Delta_{np} \qquad \sim s^0$

APPENDIX V

4^{th} Order Parameter Functions for Pb→VB

1. All of the 4^{th} order virtual momentum integrations can be reduced to the form

$$\int_0^1 ds \frac{N(x,y,z)}{C^n(M)}$$

where

$ds = dzdxdy\ z(1-z)$

n = positive integer

$N(x,y,z)$= polynomial in kinematical variables and x,y,z

and $\bar{C}(M) = A(x,z)y^2+B(x,z)y+C(x,z)$

$M=m_f$

The 4^{th} order functions $F_i(x,z)$ are the result of performing the y-integration analytically:

$$F_1(x,z)_M = \int_0^1 \frac{ydy}{\bar{C}^2} = \frac{1}{Q}\left[\frac{2A+B}{A+B+C} - BF_4(x,z)_M\right] = G_{12}(x,z)$$

$$F_2(x,z)_M = \int_0^1 \frac{y^2dy}{\bar{C}^2} = \frac{1}{Q}\left[-\frac{B+2C}{A+B+C} + 2CF_4(x,z)_M\right] = G_{22}(x,z)$$

$$F_3(x,z)_M = z^2\int_0^1 \frac{ydy}{\bar{C}} = \frac{z^2}{A}\left[\log\frac{A+B+C}{C} - BF_4(x,z)_M\right] = z^2G_{11}(x,z)$$

$$F_4(x,z)_M = \int_0^1 \frac{dy}{\bar{C}} = \frac{2}{\sqrt{Q}}\{\tan^{-1}\frac{2A+B}{\sqrt{Q}} - \tan^{-1}\frac{B}{\sqrt{Q}}\}$$

$$F_5(x,z)_M = z^2\int_0^1 \frac{y^2 dy}{\bar{C}} = \frac{z^2}{2A}[2-\frac{B}{A}\log\frac{A+B+C}{C} + \frac{B^2-2AC}{A}F_4(x,z)_M]$$

$$Q = 4AC-B^2 \qquad G_{nm}(x,z) = \int_0^1 \frac{y^m dy}{C^n(M)}$$

$N(x,y,z)$ can always be written in the form $\sum_{\ell mp} A_{\ell mp}\, x^\ell y^m z^p$. Therefore we write

$$\int_0^1 ds\, \frac{N(x,y,z)}{C^n} = \int_0^1 ds'dy \sum_{\ell mp} a_{\ell mp} \frac{x^\ell y^m z^p}{c^n(M)} = \sum_{\ell mp}\int_0^1 ds' x^\ell z^p G_{nm}(x,z)_M$$

It is usually necessary to perform the x,z integrations with help of a computer.

2. The denominators C(M)

There are three topological diagrams to consider as shown in Figure 33.

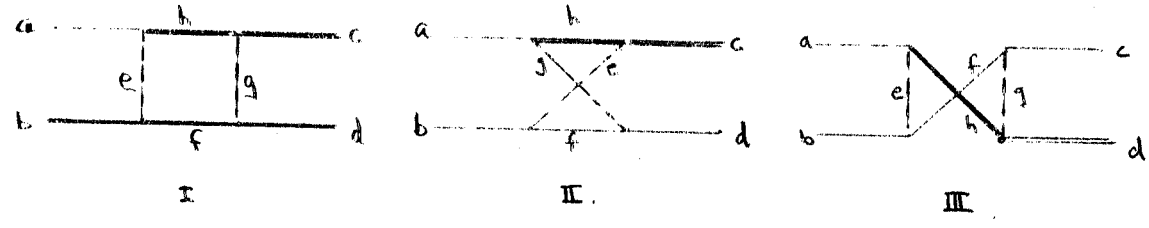

Figure 33. Configurations for two-meson exchange graphs for $\pi^+ n \to \omega p$.

(a) $\bar{C}^{I}(x,z) = A^{I}(x,z)y^2+B^{I}(x,z)y+C^{I}(x,z)$

$$A^{I}(x,z) = M_d^2 z^2$$

$$B^{I}(x,z) = (M_b^2-M_d^2-t)z^2+(M_b^2+M_c^2-s-t)z(1-z)(1-x)-(M_g^2-t)z$$

$$C^{I}(x,z) = tz^2+(M_a^2-M_c^2+t)z(1-z(1-x)+(M_g^2-t)z$$

$$+[(M_h^2-M_a^2)(1-x)+M_e^2x](1-z)+M_a^2(1-x)^2(1-z)$$

(b) $\bar{C}^{II}(x,z)$. Detailed examination of diagram II shows that exchange of a<->-c in I will give II

This leads to

$$A^{II}(x,z) = M_d^2 z^2$$

$$B^{II}(x,z) = (M_b^2-M_d^2-t)z^2+(s-M_c^2-M_d^2)z(1-z)(1-x)-(M_g^2-t)z$$

$$C^{II}(x,z) = tz^2+(M_c^2-M_a^2+t)z(1-z)(1-x)+(M_g^2-t)z$$

$$+[(M_h^2-M_c^2)(1-x)+M_e^2x](1-z)+M_c^2(1-x)^2(1-z)$$

(c) $\bar{C}^{III}(x,z)$. Similarly we get III from I via t→u and keeping labeling defined as in I (remember c,d masses interchanged here)

This gives (alternatively: use I with $\theta=\theta_{bc}$ instead of θ_{bd}

$$A^{III}(x,z) = M_d^2 z^2$$

$$B^{III}(x,z) = (M_b^2-M_d^2-u)z^2+(M_b^2+M_c^2-s-u)z(1-z)(1-x)-(M_g^2-u)z$$

$$C^{III}(x,z) = uz^2+(M_a^2-M_d^2+u)\,z(1-z)(1-x)+(M_g^2-u)$$

$$+[(M_b^2-M_a^2)(1-x)+M_e^2x](1-z)+M_a^2(1-x)^2(1-z)^2$$

Remember that only two of s,t,u are independent variables because of the relation

$$s+t+u = \sum_i M_i^2 = M_a^2+M_b^2+M_c^2+M_d^2$$

we use s and t

3. Energy Dependence

We use s and t as the independent variables. Examination of the denominator polynomials $C^I(M)$, $C^{II}(M)$, $C^{III}(M)$ gives us the s-dependence of the functions $F_i^{I,II,III}$ at fixed t.

(a) Graphs I.

$A^I(x,z)\sim s^0$ $\quad B^I(x,z)\sim s$ $\quad C^I(x,z)\sim s^0$ $\quad \rightarrow Q=4AC-B^2\sim s^2$

So we conclude

$$F_4^I(x,z)\sim s^{-1}$$

(b) Graphs II. Same as Graphs I.

(c) Graphs III. $A^{III}(x,z)\sim s^0$ $\quad B^{III}(x,z)\sim s$ $\quad C^{III}(x,z)\sim s$

$\rightarrow Q\sim as^2+bs$

and therefore

$F_4^{III}(x,z)\sim s^{-1}$ so $F_1^{III}(x,z)\sim s^{-2}$ $\quad F_3^{III}(x,z)\sim s^0$

$F_2^{III}(x,z)\sim as^{-2}+bs^{-3}$ $\quad F_5^{III}(x,z)\sim s^1$

(d) Vertex Corrections (BVB) The Diagram for this correction is shown in Figure 34.

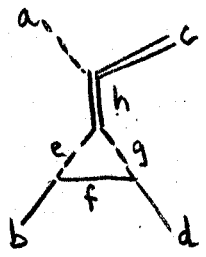

Figure 34. Configuration of NeN-vertex correction graphs for $\pi n \to \omega p$.

Since $A^I(1,z) \sim s^0$, $B^I(1,z) \sim s^0$, $C^I(1,z) \sim s^0$,

we conclude that any energy dependence vanishes from the F's at x=1:

$$F_i^I(1,z) \sim s^0,$$

and therefore, that the triangle loop cannot change the energy dependence relative to the simple BTM.